

Final report

Development of alternative in situ treatments for stony coral tissue loss disease

Principal Investigator:

Valerie J. Paul
Smithsonian Marine Station
701 Seaway Drive
Ft. Pierce, FL 34949

Collaborators:

Julie Meyer (University of Florida)
Blake Ushijima (University of North Carolina at Wilmington)
Neha Garg (Georgia Institute of Technology)

Project Dates: July 31, 2020-June 30, 2021

Prepared By:

Valerie J. Paul, Kelly A. Pitts, Paige Mandelare-Ruiz, Yesmarie De La Flor
Smithsonian Marine Station at Fort Pierce
701 Seaway Drive
Ft. Pierce, FL 34949

Jessica Deutsch and Neha Garg
School of Chemistry and Biochemistry
Georgia Institute of Technology
Atlanta, GA 30332

Introduction

Since 2014, a coral disease termed stony coral tissue loss disease (SCTLD) has spread from the Miami area to the entirety of the Florida's Coral Reef, and to numerous countries and provinces throughout the Caribbean. This highly virulent disease infects over 20 out of the 45 reef building corals of the Atlantic, resulting in massive die offs, and decreasing population densities. The etiological agents responsible for the disease are currently unknown, but mounting evidence suggests bacteria to be involved.

An investigation of the effectiveness of probiotic strain *Pseudoalteromonas* sp. McH1-7, isolated from a healthy *Montastraea cavernosa* colony, at stopping and preventing SCTLD has been conducted since 2019. Ex situ evidence has suggested McH1-7 may be an effective tool for stopping SCTLD. Additionally, methods for utilizing probiotic bacteria in the field have been developed and are showing success in early field tests.

This report summarizes Tasks 1 through 3 which aim to: 1) test methods for effective distribution of probiotics to mitigation teams and in situ deployment, 2) identify additional potential probiotics and test multi-strain probiotic treatments, and 3) develop and test diagnostic tools to complement probiotic treatments.

Task #1: To test methods for effective distribution of probiotics to mitigation teams and in situ deployment.

Traditional treatments for SCTLD have been lesion specific and do not protect the whole colony from future infections. Probiotics may allow for both direct and prophylactic treatments for SCTLD through microbial competitive exclusion.

To test in situ delivery methods using individual bagged colonies, probiotic-infused pastes, or treated coral plugs.

Whole colony bagging treatments

The trialing of whole colony probiotic treatments started in January 2020. Since then, we have determined that a plastic bag with weighted line along the bottom, analogous to spawning tents, has been effective at treating corals with probiotics off the coast of Fort Lauderdale. The bag is synched at the top to allow for ~8 cm of space between the coral and the inside of the bag to be filled with seawater. Once the bag is draped over the coral, 3.1×10^{12} cells of liquid McH1-7 culture in 50 mL of seawater is syringed into the bag via aquarium tubing (Fig.1). The syringe has a locking mechanism on it to ensure McH1-7 is not released outside of the bag. After the syringe is injected into the bag, the tubing is locked, 50 mL of seawater is taken up into the syringe, the tubing is unlocked, and then the seawater is syringed through the tubing into the bag to clear the tubing of bacteria. The tubing is removed and then the bag is left on the coral for 2 hours to allow for bacterial colonization of the coral before retrieving the bag.



Figure 1. Whole colony bagging treatment depicting a plastic bag with weighted line along the bottom draped over a coral infected with SCTLD. Liquid culture of McH1-7 is injected into the bag from a syringe via aquarium tubing. The syringe has a locking mechanism on it to prevent the bacteria from being released into the surrounding environment. The tubing is flushed with seawater before being removed from inside the bag. The bag is left over the coral for 2 h to allow for bacterial colonization of the coral. Photo by Hunter Noren, Nova Southeastern University.

To determine the viability of McH1-7 over time for transport and to ensure McH1-7 survived in syringes while transporting it to the reef, the viability of McH1-7 suspended in seawater was investigated at 5 different temperatures (-20, 4, 22 fluctuating with room temperature, 22 set in an incubator, and 28 °C). Cultures were prepared as if to be utilized in the field and were then placed in 50 mL conicals taped closed to simulate syringes. Treatment conicals were incubated at each temperature and measured for viability at 0hrs, 24hrs, 48hrs, 72hrs, and 120hrs (n=3 per treatment). Samples were taken from three separate conicals at each time point for 1:10¹-1:10⁸ dilutions using filtered seawater (FSW) in microcentrifuge tubes. Single plate serial dilution spotting from each dilution was pipetted in triplicate onto 1 SWA plate per conical replicate. Serial dilution plates for each time point were incubated for 24 hours at 28°C and a colony forming unit (CFU) count was taken from each (Fig. 2). Treatments incubated at 4 °C showed greatest potential for transportation conditions with the highest measure of bacterial viability of strain McH1-7, maintaining approximately 1x10¹⁰ CFU/mL across a 5-day period. Conditions at -20 °C also showed promise for transporting probiotic treatments, with a less than 1 log reduction in bacterial viability across time. Therefore, McH1-7 displays the greatest bacterial cell survival at low temperatures, revealing optimal storage conditions for retainment of probiotic viability for the treatment of SCTLD along the reef. This means we can be comfortable knowing the probiotic maintains viability during the few days it takes to prepare the probiotics and treat the corals in the field.

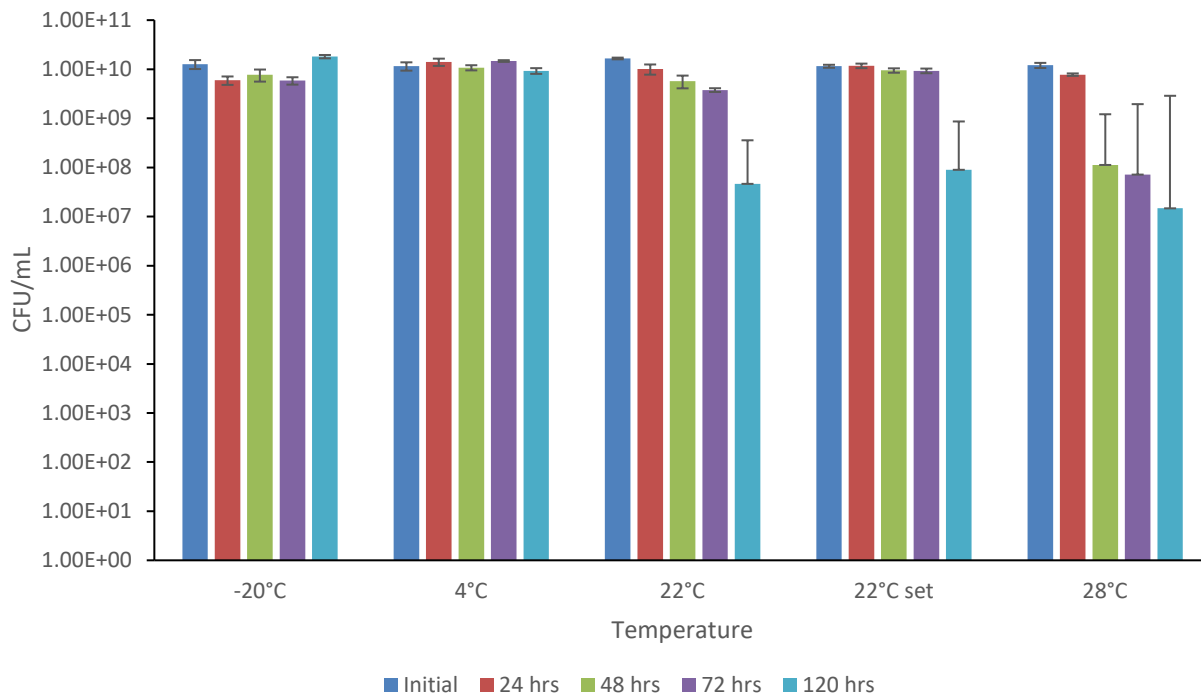


Figure 2. Average colony forming units per mL of McH1-7 after being stored at 0, 24, 48, 72, and 120 hours at 5 different temperatures. Data are shown as mean ± 1 SEM.

Lesion specific probiotic infused paste treatments

Lesion specific probiotic treatments may allow for increased microbial competitive exclusion at the lesion of infected corals. Although it is uncertain if the paste will act as a prophylactic treatment in situ, the paste allows for a faster treatment method compared to the whole colony bagging technique. Therefore, a paste, consisting of 30% polyvinylpyrrolidone (PVP), 3% sodium chloride, and 3% sodium alginate to RO water was trialed in the field starting September of 2020. The sodium alginate allows for the polymerization, or thickening, of the paste when in contact with divalent ions such as Ca^{2+} or Mg^{2+} in seawater. The paste also contains sodium chloride to avoid osmotic shock of the marine bacteria. PVP, a common ingredient in cosmetics, thickens the paste. One liter of McH1-7 with an optical density OD_{600} : 1.5 - 2 was pelleted and resuspended in 15 mL of 3% NaCl and mixed into 600 g of paste. The paste was then packed into catheter syringes at a concentration of 3.1×10^{11} cells per 50 mL syringe for transportation and use underwater (Fig. 3A). To treat corals with SCTLD, the paste was applied directly to the lesion and then flattened over top the diseased coral tissue (Fig. 3B).

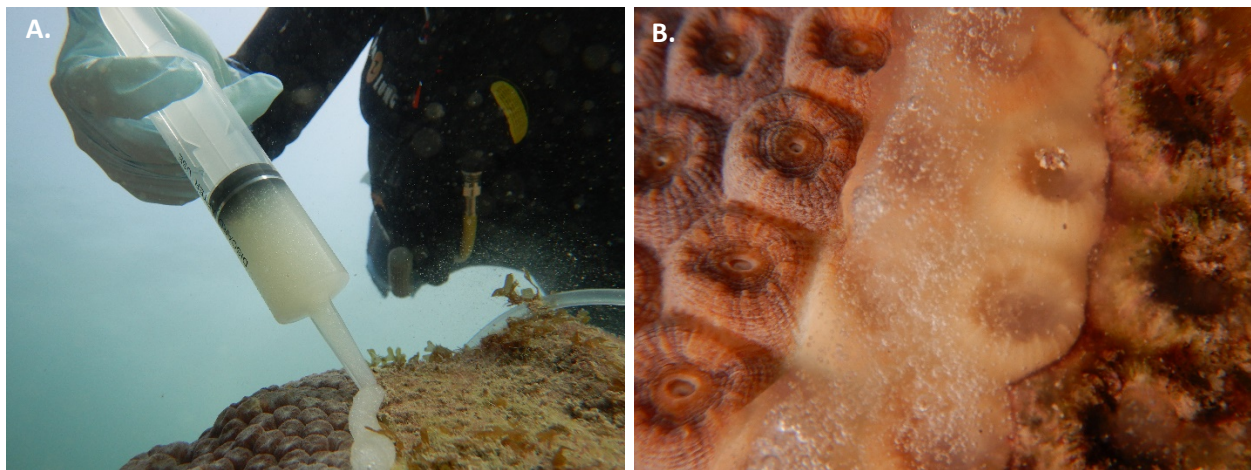


Figure 3. Probiotic paste A) being applied directly to a *Montastraea cavernosa* lesion via catheter syringe and B) covering diseased tissue until it dissolves 2 hours later. Photos by Hunter Noren, NSU.

In May of 2020, a site BS2, off the coast of Fort Lauderdale (Fig.4; $26^{\circ}9'3.1608''$ N, $80^{\circ}5'45.6828''$ W) was created by Dr. Brian Walker's lab at Nova Southeastern University (Fig. 5). A total of 21 diseased *Montastraea cavernosa* colonies were tagged, mapped and photographed. They were sampled for tissue and mucus for metabolomic and microbiome analysis on August 19, 2020 (Fig. 4). On September 1st, 8 additional corals were tagged and added to the site. Therefore, a total of 8 corals were treated on Sept. 1 with probiotic paste, 6 with a probiotic bag, 4 with control paste, 6 with a control bag, and 4 background controls that were not treated. The site was revisited on September 14th and 29th to monitor and photograph the corals. On October 14th, all corals were treated for a second time as well as 2 newly tagged corals were treated with a control bag and 4 newly tagged corals were treated with control paste

(Fig. 4). At this time, 10 corals that were completely covered in apparently healthy tissue to ensure they had not been previously infected with SCTLD were sampled for tissue and mucus as controls for metabolomic analysis. On October 30th, the site was revisited to monitor and photograph all corals. Three corals to be treated with a probiotic bag on the next treatment day were added to the site. Since the 10 corals completely covered in apparently healthy tissue were not tagged during the previous visit, a new set of 5 apparently completely healthy corals were tagged. All tagged corals at this site were sampled for tissue and mucus on Oct. 30. (See Fig. 4 for summary of sampling times.) On December 10th, all corals were photographed, and 4 newly diseased corals were tagged and added to the site to be treated with control paste, probiotic paste, or as a background control on the next treatment day. A total of 10 corals were treated with probiotic paste, 9 with a probiotic bag, 9 with control paste, 8 with a control bag, and 5 background controls on January 15th, 2021. The site was revisited on February 25th at which time 5 corals completely covered in apparently healthy tissue were tagged and sampled. The site was revisited on May 14th to photograph and monitor all colonies. All corals were 3D modeled using Agisoft Metashape Pro for photogrammetry to compare lesion progression over time. Using this software, the surface area of apparently healthy tissue as well as bleached, unhealthy tissue at the lesions was measured on every 3D model for each timepoint we visited the research site.

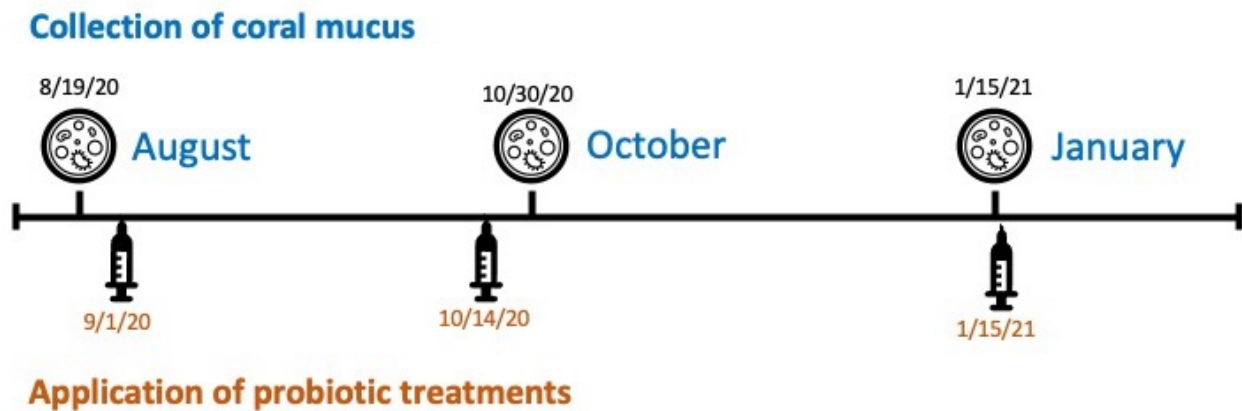


Figure 4. Timeline depicting the application of probiotic treatments to *M. cavernosa* corals and the collection of samples (coral mucus + tissue) for microbiomes and metabolomes at Broward County site BS2. Image credit: Julie Meyer, Univ. of Florida.

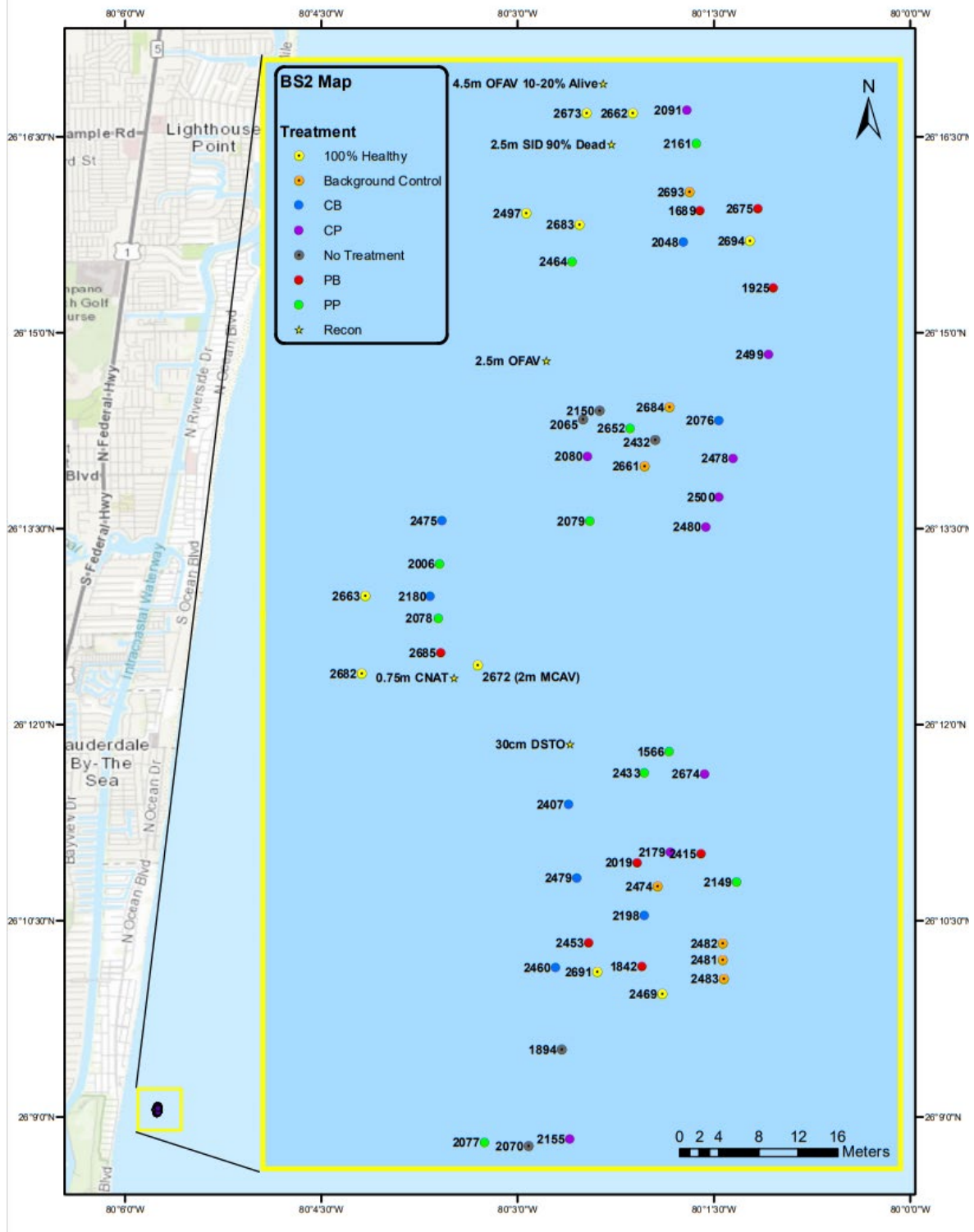


Figure 5. Map of the research site, BS2, off the coast of Fort Lauderdale depicting *M. cavernosa* colonies treated with probiotic paste (green), probiotic bag (red), control paste (purple), control bag (blue), or as a background control (orange) or corals that were completely covered in apparently healthy tissue (yellow). Map created by Sammi Buckley, NSU.

Each colony at the research site was categorized into 1 of 5 health statuses based on the results of the 3D modeling from February 25th, 2021, after most corals had been treated 3 times (Figs. 4, 6): Healing = bleached tissue is regaining symbiotic microalgae and pigmentation, stopped: the disease has stopped progressing across the coral and tissue loss has stopped, chronic tissue loss = the disease is slowly progressing across the coral, active tissue loss = the disease is quickly progressing across the coral, dead = all of the tissue on the colony has died. There is a significant association between health status and treatment for these categories (Fisher exact test: $p = 0.0017$). As demonstrated by the shading of Pearson’s residuals in a mosaic plot, corals that were treated with the probiotic bag were more likely to be healing and background control corals were more likely to have died than would be expected if the model was fully independent (Fig. 7; sum of squares test, $p=0.0016$).

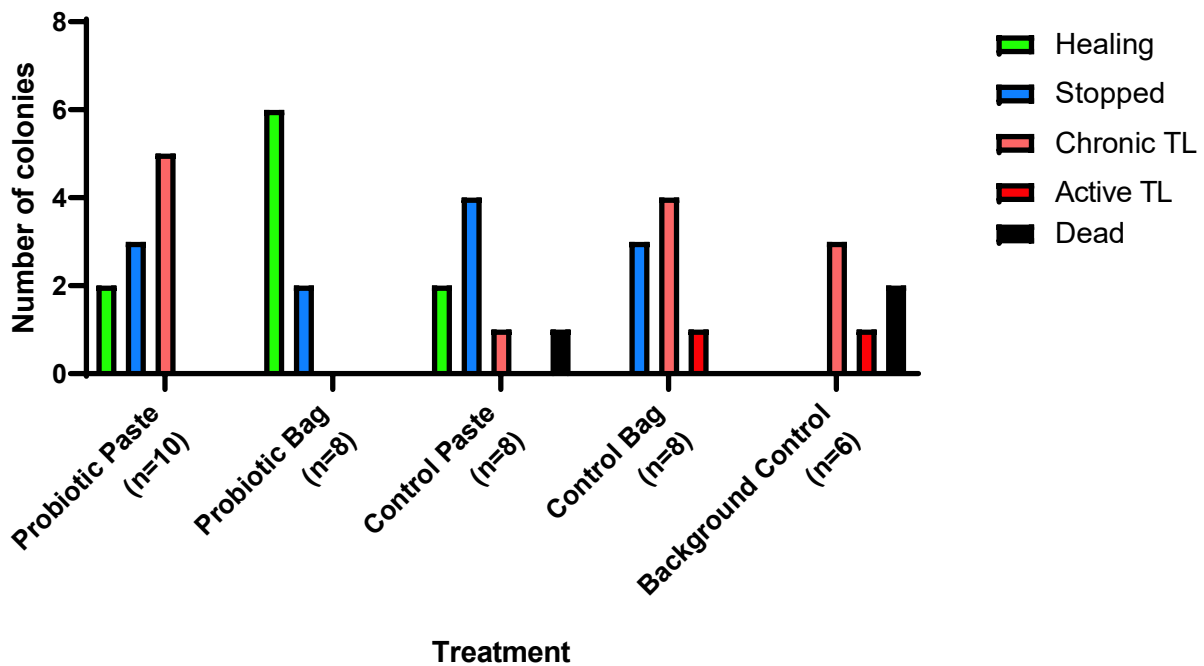


Figure 6. Number of coral colonies healing (green), with stopped lesion progression (blue), slow lesion progression (pink), fast lesion progression (red), or completely dead (black) based on the treatment they received.

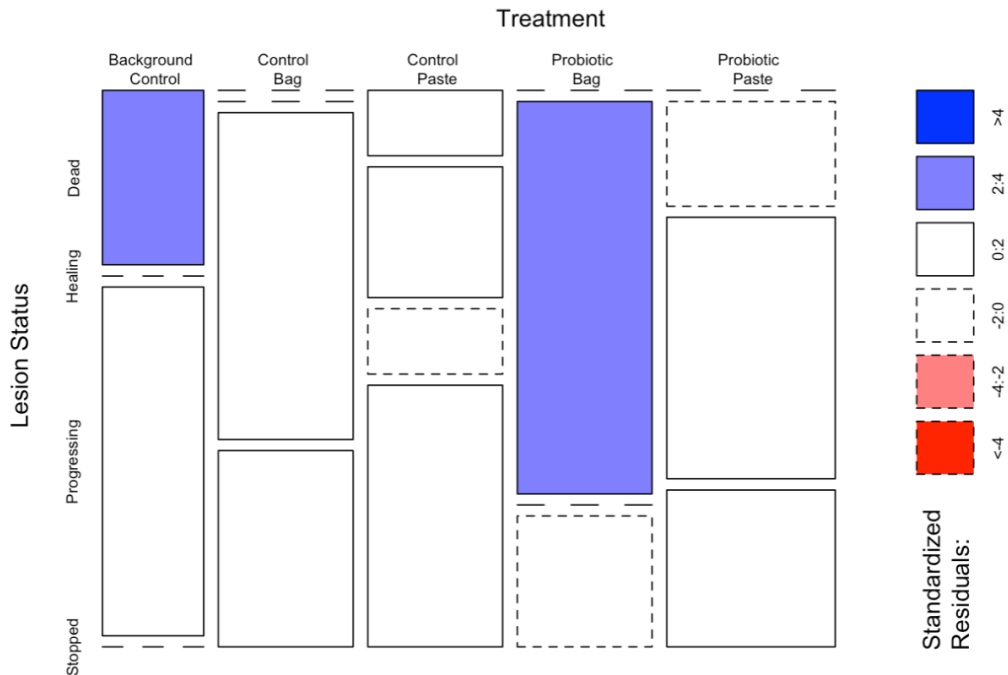


Figure 7. Pearson's mosaic plot showing differences in coral health status based on treatment type. Blue residuals mean there are more observations in that cell than would be expected under the null model. Therefore, corals that were treated with the probiotic bag were more likely to be healing and background control corals were more likely to have died, than would be expected if the model was fully independent.

A new research site, Mk48-5 (Fig. 7; 24°41'14.964" N, 81°2'25.044" W), was established outside of Marathon, FL, on May 12th, 2021 with the help of Dr. Karen Neely and her dive team (Fig. 8). This site was created to determine if the use of both a probiotic bag and probiotic paste treatment simultaneously would be more effective at stopping and preventing SCTLD and to test the effectiveness of McH1-7 on corals in the FL Keys. A total of 17 *M. cavernosa* and 4 *Colpophyllia natans* colonies were treated with probiotics by putting probiotic paste directly on the lesion and then covering the whole colony with a bag and injecting it with McH1-7 according to the methodologies above. Similarly, 18 *M. cavernosa* and 4 *C. natans* colonies were treated as controls using the same paste and bagging technique, absent of probiotics. Six *M. cavernosa* colonies were treated as background controls in which they were not treated but are to be monitored over time. All colonies were tagged, photographed, and sampled for tissue and mucus for metabolomic analysis before treatment. Using these photos, 3D models of each colony will be created to compare disease progression over time.

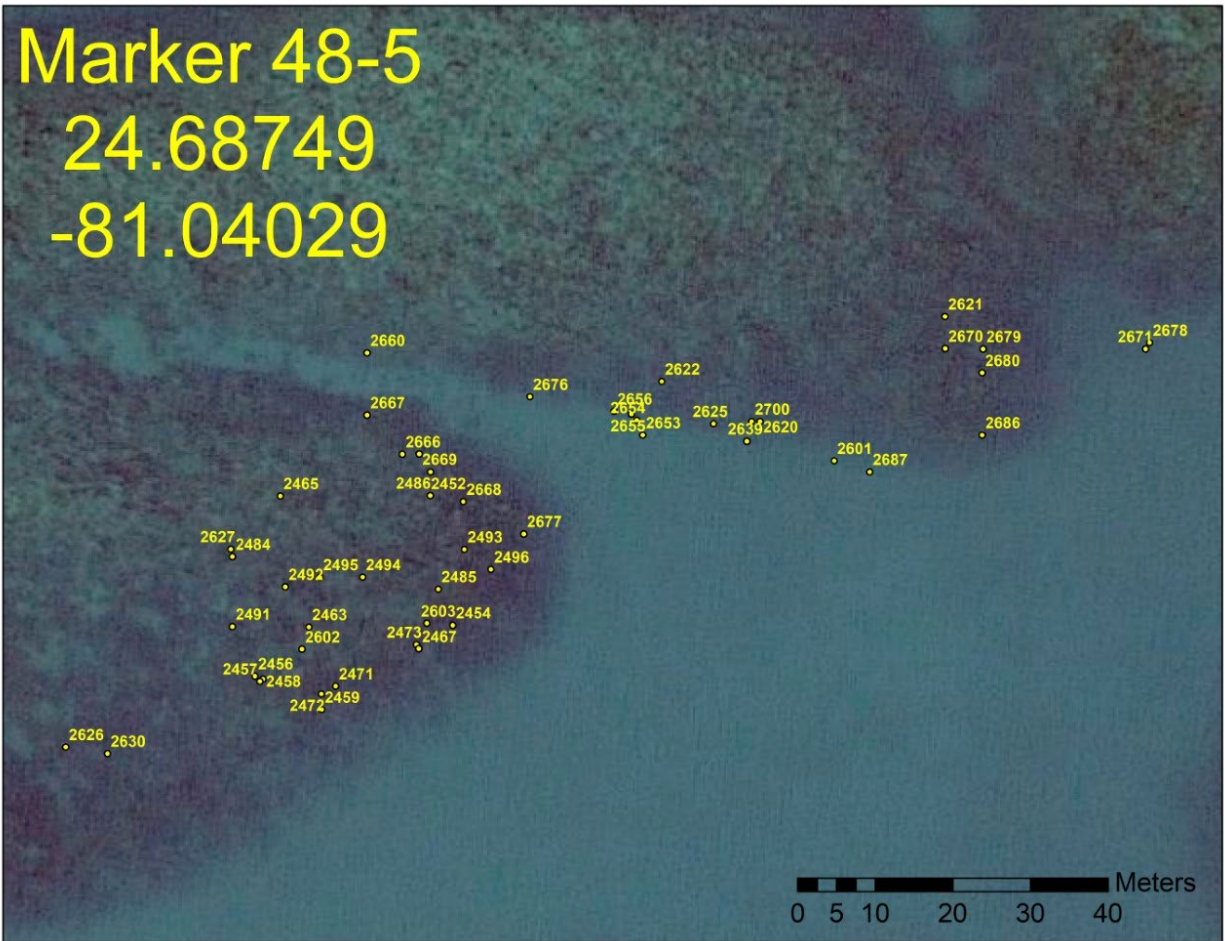


Figure 8. Research site Mk48-5 outside of Marathon, Florida including 41 *M. cavernosa* colonies and 8 *C. natans* colonies. Map created by Karen Neely, NSU.

Research site Mk48-5 in the Keys is typically exposed to more surge than BS2 outside of Fort Lauderdale and was therefore harder to treat effectively. The movement of the water was knocking the treatment bag back and forth, inevitably pulling the paste off the lesion underneath. Treatment bags were also difficult to keep directly over the coral lesion without the bottom of the bag opening or the bag shifting off the coral. Heavier bags weighted with chain may be more effective at staying in place. We also plan to treat the coral with the bag before treating the lesion with the paste in the future to avoid collision between the two.

To determine the least amount of in situ treatments required to stop disease lesions and the duration that treatment can potentially protect against infection.

The ability of probiotics to act as either a prophylactic or direct treatment may greatly depend on the ability of the bacteria to persist as part of the coral's holobiont overtime. It is currently unknown how often corals on the reef require treatment with probiotics to stop SCTL progression. Corals at BS2 were treated up to 3 times depending on when they became diseased and were added to the site. The total surface area of tissue (cm²) lost over time was calculated using Agisoft Metashape Pro and graphed (Fig. 9; two-way ANOVA: p = 0.0011). The probiotic

bag (Tukey's post hoc: $p = 0.004$) and control paste (Tukey's post hoc: $p = 0.011$) treatments significantly differed from the background control treatment. All other comparisons between treatments were not significant. It appears that tissue loss on corals treated with a probiotic bag remained stable and was smaller than most treatments after the second treatment in October. However, a greater sample size of treated corals is necessary to further investigate how many treatments are required for effectively stopping SCTL D.

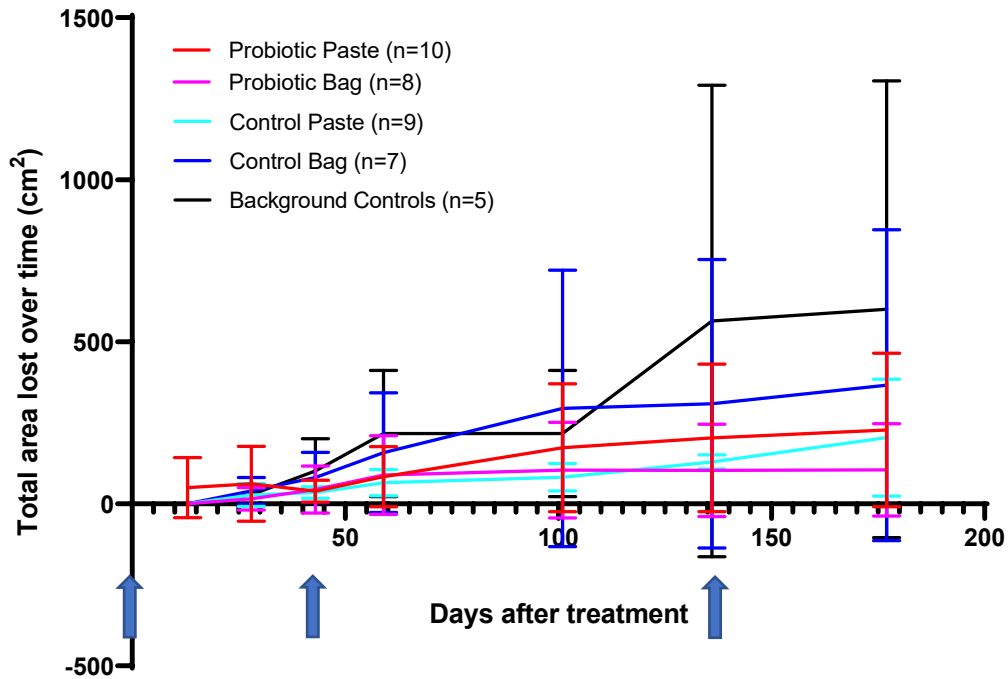


Figure 9. Total tissue surface area (cm^2) lost on corals at BS2 overtime. Corals were treated on day 0, 43, and 136 (blue arrows). Data are shown as mean \pm 1 SEM.

The surface area of visibly healthy tissue remaining showing no signs of bleaching was also calculated using Agisoft Metashape Pro (Fig. 10; two-way ANOVA: $p = 0.032$); however, there were no significant differences between any two treatments. It appears that the healthy tissue on colonies treated with a probiotic bag or paste has remained stable over time. The trend from this data suggests that the tissue lost on these corals is not healthy tissue, but instead tissue that was already bleaching and diseased. However, a greater sample size is required to determine any significant differences between treatments.

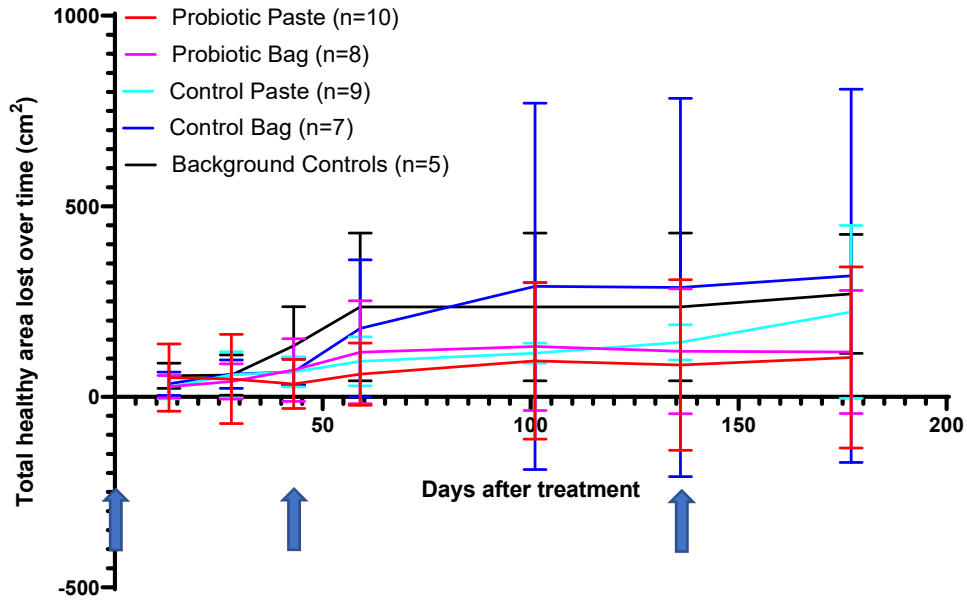


Figure 10. Total healthy tissue surface area (cm^2) lost on corals at BS2 overtime. Corals were treated on day 0, 43, and 136 (blue arrows). Data are shown as mean \pm 1 SEM.

To test lyophilization protocols to enhance transportation and distribution of probiotic treatments.

Working with live bacteria presents a challenge when transporting probiotics into the field for use on corals infected with SCTLD. Lyophilization, or freeze drying, would allow for long term storage of McH1-7 at room temperature for easier preparation and transportation of the probiotic. To investigate best practices for lyophilization, McH1-7 culture was aliquoted into pre-weighed 50 mL conicals in triplicate. One extra 50 mL conical was prepared for the purposes of the indicator solution which would show if the culture was properly freeze dried. Conical cultures were spun down at 8,000 rpm for 10 minutes and supernatant was decanted. The culture was weighed to obtain pellet mass in grams. The pellet was then resuspended in 1:1 volume Microbial Freeze-Drying Buffer and mixed thoroughly. Replicates were incubated at -80°C for two hours and then freeze dried for 15 hours. Freeze dried pellet formed. Freeze dried bacteria was placed at room temp storage for 18 days and continues to have maintained freeze-dried state (Fig. 11). We still need to determine how long these are viable.



Figure 11. From left to right: Indicator solution to ensure proper lyophilization and three vials of McH1-7 still lyophilized after 18 days of sitting at room temperature.

To test the potential binding to food (live or dried) to enhance probiotic uptake or delivery.

There has been histological evidence of SCTLD originating from inner layers of coral tissue. Ingestion of McH1-7 may allow for the colonization of bacteria within the gastrointestinal cavity, permitting probiotics to penetrate deeper tissue. Mote Marine Laboratory IC2R3 at Summerland Key observed tissue loss within five of their tables holding *M. cavernosa* and *O. faveolata* colonies. McH1-7 in liquid culture was sent to Mote to treat four of these tables by mixing the probiotic directly with food and adding both to the table. The corals tolerated this well, and in one case, for a sea table that had been previously dosed with antibiotics, the follow-up treatment with probiotics greatly decreased the tissue loss that was observed in the tank before probiotic treatment.

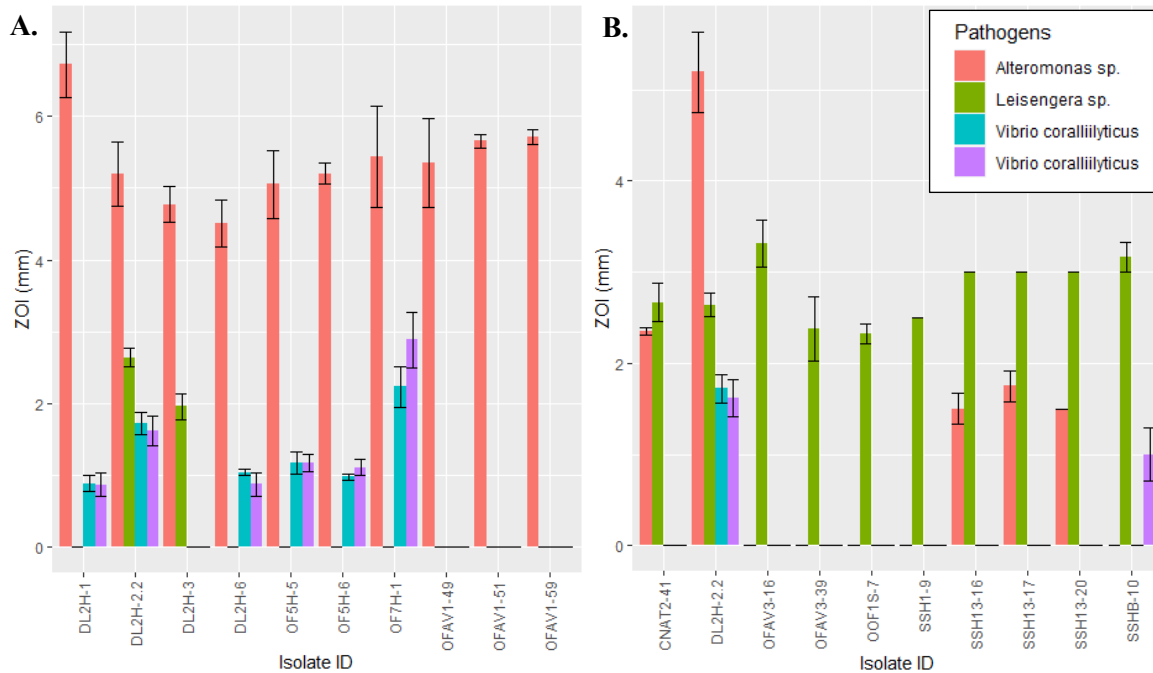
Task #2: To identify additional potential probiotics and test multi-strain probiotic treatments.

To screen at least 300 isolates against a panel of putative pathogens in the laboratory.

A total of 600 new isolates grown on seawater agar have been screened for inhibitory activity against putative pathogens. Of these, 96 isolates have been further pursued as promising candidates for probiotic development based on demonstrated inhibitory activity against at least one of the target pathogenic strains (*Leisingera* sp. McT4-56, *Alteromonas* sp. McT4-15, *Vibrio coralliilyticus* OfT6-21 or OfT7-21) (Fig. 12, Table 1). We were particularly interested in the isolates targeting *Vibrio coralliilyticus* because it can coinfect corals with SCTLD and increase rates of tissue loss, therefore we tested two different strains of this pathogen. Each putative pathogen was grown in seawater broth (SWB, typtone, yeast, and FSW) at 28 °C and 150 RPM for 48 hours. Sterile tips were used to pick single bacterial isolate colonies and the colonies were placed in 96 well plates with 214 µL of SWB for 48 hours at 28 °C and 150 RPM. Optical density readings at 600 nm were obtained on the bacteria isolates at 24 and 48 hours and

200µL of the diluted pathogens were placed onto SWA plates. The plated pathogens were allowed to dry on the plate for 15 minutes before adding the bacterial isolates. 10.0µL of the bacterial isolates were plated on the pathogen-enriched SWA plate, in designated spaces. The bacterial isolates were dried onto the SWA plate for 30 minutes before placing in the 28 °C incubator for 24 hours. After 24 hours, zones of inhibition (ZOIs) were scored as partial (cloudy, not clear) or complete (clear).

Active isolates were sequenced for 16S rRNA gene for taxonomic identification. Isolates with the largest zones of inhibition against multiple pathogens were further considered for trialing on corals with SCTLD in the laboratory. These were also sent to Dr. Julie Meyer’s laboratory, University of Florida, to sequence the genomes. Additionally, priority strains were grown for chemical analysis by LC-MS by Dr. Neha Garg’s laboratory at Georgia Tech.



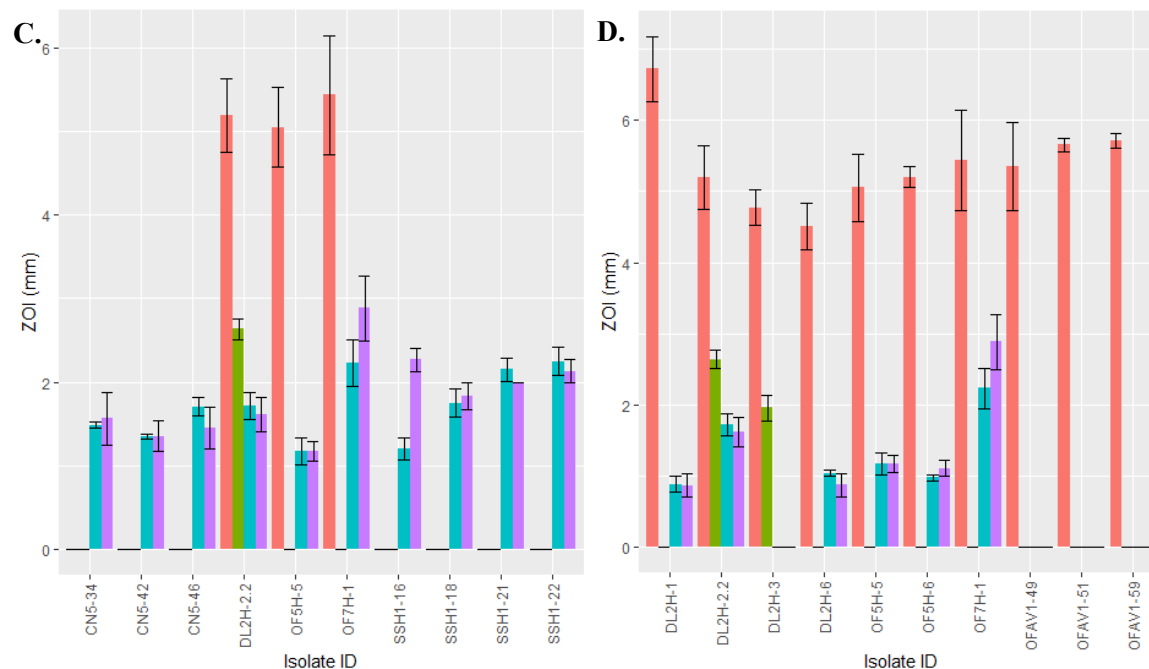


Figure 12. Bioactivity assays showing the top 10 isolates that displayed the largest zones of inhibition against A) *Alteromonas sp.* McT4-15, B) *Leisingera sp.* McT4-56, C) *Vibrio corallilyticus* (blue OfT6-21, purple OfT7-21), and D) the most active across all 4 pathogenic strains.

Table 1. Average zones of inhibition (mm) of isolates plated against putative pathogens. Test strains are *Alteromonas sp.* McT4-15, *Leisingera sp.* McT4-56, and two strains of *Vibrio corallilyticus* (OfT6-21, OfT7-21). Larger zones of inhibition are displayed in darker shades of red.

Isolate ID	Species	Date of Testing	McT4-15		McT4-56		OfT6-21		OfT7-21	
			Mean	St.Err.	Mean	St.Err.	Mean	St.Err.	Mean	St.Err.
OF3S-11	<i>Vibrio fortis</i>	7/24/2021	0.00	0.00	0.00	0.00	0.00	0.00	0.00	0.00
OOF1S-7	<i>Pseudoalteromonas rubra</i>	7/24/2021	0.00	0.00	2.32	0.11	0.00	0.00	0.00	0.00
OOF1S-3	<i>Vibrio corallilyticus</i>	7/24/2021	3.27	0.15	0.00	0.00	0.00	0.00	0.00	0.00
OOF2S-9	<i>Tenacibaculum skagerrakense</i>	7/24/2021	0.00	0.00	0.00	0.00	0.00	0.00	0.00	0.00
SSOF7-84	<i>Vibrio sinaloensis</i>	7/24/2021	0.00	0.00	0.00	0.00	0.00	0.00	0.00	0.00
SSOF7-85	<i>Vibrio tubiashii</i>	7/24/2021	0.00	0.00	1.12	0.09	0.00	0.00	0.00	0.00
SSOF7-88	<i>Vibrio tubiashii</i>	7/24/2021	0.00	0.00	0.00	0.00	0.00	0.00	0.00	0.00
OFAV1-3	<i>Thalassotalea euphylliae</i>	7/24/2021	0.00	0.00	0.00	0.00	0.00	0.00	0.00	0.00
OFAV1-8	<i>Epibacterium mobile</i>	7/24/2021	1.37	0.13	2.12	0.10	1.00	0.00	0.00	0.00
OFAV1-13	<i>Thalassotalea euphylliae</i>	7/24/2021	0.00	0.00	0.00	0.00	0.00	0.00	0.00	0.00
OFAV1-16	<i>Labrenzia aggregata</i>	7/24/2021	0.00	0.00	0.00	0.00	0.00	0.00	0.00	0.00
OFAV1-18	<i>Labrenzia aggregata</i>	7/24/2021	0.00	0.00	0.00	0.00	0.00	0.00	0.00	0.00
OFAV2-16	<i>Ruegeria atlantica</i>	7/24/2021	1.28	0.12	0.00	0.00	0.00	0.00	0.00	0.00
OFAV1-49	<i>Vibrio harveyi</i>	7/24/2021	5.35	0.62	0.00	0.00	0.00	0.00	0.00	0.00
OFAV1-51	<i>Vibrio harveyi</i>	7/24/2021	5.65	0.09	0.00	0.00	0.00	0.00	0.00	0.00
OFAV1-59	<i>Vibrio harveyi</i>	7/24/2021	5.72	0.11	0.00	0.00	0.00	0.00	0.00	0.00

OFAV2-2	<i>Ruegeria arenilitoris</i>	7/24/2021	0.00	0.00	0.00	0.00	0.00	0.00	0.00	0.00
OFAV2-6	<i>Ruegeria arenilitoris</i>	7/24/2021	0.00	0.00	0.00	0.00	0.00	0.00	0.00	0.00
OFAV2-7	<i>Photobacterium marinum</i>	7/24/2021	0.00	0.00	0.00	0.00	0.00	0.00	0.00	0.00
OFAV2-19	<i>Thalassotalea euphylliae</i>	8/5/2020	0.00	0.00	2.29	0.01	0.00	0.00	0.00	0.00
OFAV2-20	<i>Vibrio harveyi</i>	8/5/2020	0.00	0.00	2.27	0.44	0.00	0.00	0.00	0.00
OFAV2-48	<i>Vibrio tubiashii</i>	8/5/2020	0.00	0.00	0.00	0.00	0.00	0.00	0.00	0.00
OFAV3-4	<i>Vibrio harveyi</i>	8/5/2020	0.00	0.00	0.00	0.00	0.00	0.00	0.00	0.00
OFAV3-8	<i>Vibrio harveyi</i>	8/5/2020	0.00	0.00	0.00	0.00	0.00	0.00	0.00	0.00
OFAV3-11	<i>Vibrio harveyi</i>	8/5/2020	0.00	0.00	0.00	0.00	0.00	0.00	0.00	0.00
OFAV3-16	<i>Thalassotalea euphylliae</i>	8/5/2020	0.00	0.00	3.31	0.25	0.00	0.00	0.00	0.00
OFAV3-39	<i>Ruegeria conchae</i>	8/5/2020	0.00	0.00	2.38	0.35	0.00	0.00	0.00	0.00
OFAV3-42	<i>Ruegeria atlantica</i>	8/5/2020	0.00	0.00	0.00	0.00	0.00	0.00	0.00	0.00
DL2H-1	<i>Pseudoalteromonas rubra</i>	10/16/2020	6.72	0.46	0.00	0.00	0.89	0.12	0.87	0.16
DL2H-6	<i>Pseudoalteromonas piscicida</i>	10/16/2020	4.51	0.33	0.00	0.00	1.04	0.05	0.88	0.16
OF5H-2	<i>Vibrio owensii</i>	10/16/2020	0.79	0.01	0.00	0.00	0.00	0.00	0.00	0.00
OF5H-3	<i>Vibrio alginolyticus</i>	10/16/2020	0.71	0.13	0.00	0.00	0.00	0.00	0.00	0.00
OF5H-5	<i>Pseudoalteromonas piscicida</i>	10/16/2020	5.05	0.48	0.00	0.00	1.18	0.16	1.17	0.12
OF5H-6	<i>Pseudoalteromonas piscicida</i>	10/16/2020	5.20	0.15	0.00	0.00	0.98	0.04	1.11	0.12
OF5H-8	<i>Vibrio alginolyticus</i>	10/16/2020	0.00	0.00	0.00	0.00	0.00	0.00	0.00	0.00
Ss3H-1	<i>Vibrio harveyi</i>	10/16/2020	0.00	0.00	0.00	0.00	0.00	0.00	0.00	0.00
Ss3H-2	<i>Vibrio harveyi</i>	10/16/2020	0.00	0.00	0.00	0.00	0.00	0.00	0.00	0.00
Ps1H-2	<i>Vibrio owensii</i>	10/16/2020	0.74	0.03	0.00	0.00	0.00	0.00	0.00	0.00
Ps1H-9	<i>Vibrio rotiferianus</i>	10/16/2020	0.00	0.00	0.00	0.00	0.00	0.00	0.00	0.00
Ps1H-14	<i>Alteromonas australica</i>	10/16/2020	0.00	0.00	0.00	0.00	0.00	0.00	0.00	0.00
DL2H-2.2	<i>Pseudoalteromonas rubra</i>	10/16/2020	5.20	0.44	2.64	0.13	1.72	0.16	1.62	0.20
DL2H-3	<i>Pseudoalteromonas rubra</i>	10/16/2020	4.77	0.25	1.96	0.18	0.00	0.00	0.00	0.00
MC1H-2	<i>Vibrio harveyi</i>	10/16/2020	0.00	0.00	0.00	0.00	0.00	0.00	0.00	0.00
OF7H-1	<i>Pseudoalteromonas piscicida</i>	10/16/2020	5.44	0.71	0.00	0.00	2.23	0.28	2.89	0.39
CNAT2-1	<i>Vibrio owensii</i>	1/7/2021	0.58	0.02	0.54	0.06	0.00	0.00	0.00	0.00
CNAT2-7	<i>Vibrio rotiferianus</i>	1/7/2021	0.51	0.05	0.56	0.03	0.00	0.00	0.00	0.00
CNAT2-8	<i>Alteromonas macleodii</i>	1/7/2021	0.00	0.00	0.00	0.00	0.00	0.00	0.00	0.00
CNAT2-9	<i>Pseudoalteromonas ruthenica</i>	1/7/2021	2.56	0.36	1.00	0.02	0.00	0.00	0.00	0.00
CNAT2-13	<i>Pseudoalteromonas ruthenica</i>	1/7/2021	2.58	0.21	0.00	0.00	0.00	0.00	0.00	0.00
CNAT2-16	<i>Pseudoalteromonas piratica</i>	1/7/2021	0.00	0.00	0.00	0.00	0.00	0.00	0.00	0.00
CNAT2-18	<i>Pseudoalteromonas ruthenica</i>	1/7/2021	2.35	0.19	1.10	0.02	0.00	0.00	0.00	0.00
CNAT2-19	<i>Alteromonas macleodii</i>	1/7/2021	0.00	0.00	0.00	0.00	0.00	0.00	0.00	0.00
CNAT2-25	<i>Ruegeria conchae</i>	1/7/2021	0.86	0.02	0.99	0.10	0.00	0.00	0.00	0.00
CNAT2-28	<i>Epibacterium mobile</i>	1/7/2021	0.00	0.00	0.00	0.00	0.00	0.00	0.00	0.00
CNAT2-31	<i>Escherichia fergusonii</i>	1/7/2021	0.47	0.01	1.01	0.12	0.00	0.00	0.00	0.00
CNAT2-35	<i>Alteromonas macleodii</i>	1/7/2021	0.00	0.00	0.00	0.00	0.00	0.00	0.00	0.00
CNAT2-40	<i>Alteromonas macleodii</i>	1/7/2021	0.00	0.00	0.00	0.00	0.00	0.00	0.00	0.00

CNAT2-41	<i>Pseudoalteromonas ruthenica</i>	1/7/2021	2.35	0.04	2.67	0.21	0.00	0.00	0.00	0.00
CNAT2-43	<i>Pseudovibrio denitrificans</i>	1/7/2021	0.00	0.00	0.89	0.08	0.00	0.00	0.00	0.00
CNAT2-44	<i>Tenacibaculum geojense</i>	1/7/2021	0.00	0.00	0.00	0.00	0.00	0.00	0.00	0.00
CNAT2-45	<i>Tenacibaculum geojense</i>	1/7/2021	0.00	0.00	0.00	0.00	0.00	0.00	0.00	0.00
CNAT3-17	<i>Alteromonas macleodii</i>	1/7/2021	0.00	0.00	0.00	0.00	1.24	0.14	0.00	0.00
CNAT3-28	<i>Alteromonas macleodii</i>	1/7/2021	0.00	0.00	0.00	0.00	1.25	0.27	0.00	0.00
MCAV2-41	<i>Aquimarina salinaria</i>	1/27/2021	0.00	0.00	0.00	0.00	0.00	0.00	0.00	0.00
MCAV3-45	<i>Epibacterium mobile</i>	1/27/2021	0.00	0.00	0.00	0.00	0.00	0.00	0.00	0.00
MCAV3-52	<i>Tenacibaculum mesophilum</i>	1/27/2021	0.53	0.07	0.86	0.04	0.00	0.00	0.00	0.00
CN5-1	<i>Tenacibaculum aiptasiae</i>	2/26/2021	0.00	0.00	0.00	0.00	1.40	0.15	0.00	0.00
CN5-10	<i>Vibrio sinaloensis</i>	2/26/2021	0.00	0.00	0.00	0.00	1.10	0.07	0.00	0.00
CN5-12	<i>Halomonas meridiana</i>	2/26/2021	2.06	0.31	0.00	0.00	0.00	0.00	0.00	0.00
CN5-34	<i>Tenacibaculum aiptasiae</i>	2/26/2021	0.00	0.00	0.00	0.00	1.49	0.04	1.56	0.31
CN5-37	<i>Pseudoalteromonas shioyasakiensis</i>	2/26/2021	0.00	0.00	1.90	0.31	0.00	0.00	0.00	0.00
CN5-42	<i>Thalassobius mediterraneus</i>	2/26/2021	0.00	0.00	0.00	0.00	1.35	0.03	1.36	0.18
CN5-46	<i>Tenacibaculum aiptasiae</i>	2/26/2021	0.00	0.00	0.00	0.00	1.71	0.11	1.46	0.25
PAST1-8	<i>Photobacterium rosenbergii</i>	2/26/2021	0.00	0.00	0.00	0.00	0.00	0.00	0.00	0.00
PAST1-9	<i>Vibrio maritimus</i>	2/26/2021	0.00	0.00	1.20	0.06	0.00	0.00	0.00	0.00
PAST1-11	<i>Vibrio maritimus</i>	2/26/2021	0.00	0.00	0.00	0.00	0.00	0.00	0.00	0.00
PAST1-19	<i>Vibrio alginolyticus</i>	2/26/2021	1.39	0.08	1.31	0.06	0.00	0.00	0.00	0.00
PAST1-21	<i>Vibrio fortis</i>	2/26/2021	1.73	0.10	0.00	0.00	0.00	0.00	0.00	0.00
SSH1-6	<i>Tenacibaculum mesophilum</i>	4/30/2021	0.00	0.00	0.00	0.00	0.00	0.00	1.93	0.23
SSH1-9	<i>Tenacibaculum mesophilum</i>	4/30/2021	0.00	0.00	2.50	0.00	0.00	0.00	0.00	0.00
SSH1-11	<i>Tenacibaculum mesophilum</i>	4/30/2021	0.00	0.00	2.00	0.00	0.00	0.00	0.00	0.00
SSH1-16	<i>Tenacibaculum mesophilum</i>	4/30/2021	0.00	0.00	0.00	0.00	1.20	0.13	2.27	0.15
SSH1-18	Not yet determined	4/30/2021	0.00	0.00	0.00	0.00	1.75	0.17	1.83	0.17
SSH1-21	Not yet determined	4/30/2021	0.00	0.00	0.00	0.00	2.15	0.15	2.00	0.00
SSH1-22	<i>Tenacibaculum mesophilum</i>	4/30/2021	0.00	0.00	0.00	0.00	2.25	0.17	2.13	0.13
SSH13-16	<i>Vibrio harveyi</i>	4/30/2021	1.50	0.17	3.00	0.00	0.00	0.00	0.00	0.00
SSH13-20	<i>Vibrio harveyi</i>	4/30/2021	1.50	0.00	3.00	0.00	0.00	0.00	0.00	0.00
SSH13-17	<i>Vibrio harveyi</i>	4/30/2021	1.75	0.17	3.00	0.00	0.00	0.00	0.00	0.00
SSHB-1	<i>Leisingera caerulea</i>	4/30/2021	0.00	0.00	0.00	0.00	0.00	0.00	0.00	0.00
SSHB-2	<i>Leisingera caerulea</i>	4/30/2021	0.00	0.00	0.00	0.00	0.00	0.00	0.00	0.00
SSHB-10	<i>Vibrio alginolyticus</i>	4/30/2021	0.00	0.00	3.17	0.17	0.00	0.00	1.00	0.29
SSHB-14	<i>Pseudoalteromonas piratica</i>	4/30/2021	0.00	0.00	0.00	0.00	0.00	0.00	0.00	0.00
SSHB-22	<i>Leisingera caerulea</i>	4/30/2021	0.00	0.00	0.00	0.00	0.00	0.00	0.00	0.00
SSHB-23	<i>Leisingera caerulea</i>	4/30/2021	0.00	0.00	0.00	0.00	0.00	0.00	0.00	0.00
SSHB-25	<i>Leisingera caerulea</i>	4/30/2021	0.00	0.00	0.00	0.00	0.00	0.00	0.00	0.00

In addition to these standard growth conditions, Smithsonian Postdoctoral Fellow Dr. Paige Mandelare-Ruiz has been working on isolating coral-associated bacteria with alternate media types to focus on more slow growing bacteria and to target different taxonomic groups such as Actinobacteria that are known for their antibiotic properties.

Established sampling techniques were utilized for sampling mucus and tissue. A 30cc syringe was used to obtain the mucus and ~15mL of mucus/water was obtained. Corals with visible SCTLD lesions were sampled twice, once at the diseased lesion divide and a second sampling at visibly healthy tissue. Healthy corals were sampled once at the visibly healthy tissue. Mucus samples were stored at 4 °C until plating. Cycloheximide (inhibits yeast and most environmental ascomycetes, cyclo) and nalidixic acid (inhibits environmental bacteria contaminants, such as *Enterobacter* spp. and *Escherichia coli*, nali) concentrations and trace-element solution were obtained from ActinoBase. The isolation media used in this study were the following: International Streptomyces Project-2 agar (ISP-2), M1 agar, Actinomycete Isolation Agar (AIA, premade mixture from BD Difco™), Zobell Marine Agar 2216 Plus (ZMb+), Soy Flour Mannitol agar (SFM), Marine Broth (MB), 10% strength, Minimal Medium (MM), and NaST21Cx Agar. Isolation media consisted of the following: ISP-2, 4g yeast extract, 10g malt extract, 4g dextrose, 20g agar, 1mL trace element solution, and 1L FSW; M1, 10g starch, 4g yeast extract, 2g peptone, 18g agar, 1mL trace element solution, and 1L FSW; AIA, 22.0g pre-mixed ingredients, 18g glycerol, and 50:50 reverse osmosis water:FSW; ZMb+, 4.0g Difco marine broth, 36g InstantOcean® salts, 2.0g sodium nitrate, 15g agar, and 1L ultra-pure water; SFM, 20g mannitol, 20g soy flour, 20g agar, 1mL trace element solution, and 1L FSW; MB, 10% of the pre-made mixture per 1L FSW; MM, AIA pre-made mix 22.0g, 5g mannitol, 5mL glycerol, and 1L FSW; and NaST21Cx, solution A (750mL FSW, 1g dipotassium phosphate, 10g agar) and solution B (250mL FSW, 1g potassium nitrate, 1g magnesium sulphate, 1g calcium chloride, dihydrate, 0.2g iron(III) chloride, and 0.1g manganese sulphate, heptahydrate), mixed together after autoclaving. All coral mucus, coral tissue in FSW, and water concentrate samples were heat treated in a 55°C water bath for 5 minutes. Water Concentrate was plated on the listed isolation agars at 10.0 µL and coral mucus and coral tissue in seawater was plated on the listed isolation agars at 25.0 µL. Bacteria colonies were isolated by interesting color and morphology, natural zones of inhibition, and time of growth (greater than one week of growth). Selected colonies were plated on their respective isolation antibiotic agar once to ensure purity of strain followed by a final passage onto seawater agar (SWA, tryptone, yeast, agar, and FSW) to maintain collection.

Since joining the Smithsonian Marine Station in March, Paige has obtained over 375 new isolates using these methods, with 176 of those screened against three pathogen strains. Forty-five strains have shown activity and some of these will warrant further follow up by chemical studies and possible tests with live corals in aquarium assays. Nine Actinobacteria strains are of interest and will be further studied for their antimicrobial properties.

To advance at least three of the most promising isolates to aquarium trials with diseased corals.

This investigation of potential probiotics was continued on coral colonies in the laboratory by inoculating diseased fragments in aquaria weekly and monitoring disease progression for 21-32 days. For comparison of effectiveness, most strain trials were conducted concurrently with

McH1-7 as this strain previously demonstrated effectiveness in trials conducted from 2018-2020. Therefore, colonies of the same genotype were treated with filtered seawater (control), McH1-7, and other strains tested at time of trial.

Effectiveness of probiotic strains McH1-25 and CnMc7-37 at treating infected Montastraea cavernosa colonies

Two potential probiotic strains isolated from healthy *M. cavernosa* colonies, McH1-25 and CnMc7-37, produced zones of inhibition against putative pathogens in last year's tests and were therefore trialed on *M. cavernosa* colonies. A total of five genotypes were split evenly into fragments to be inoculated with either McH1-7, McH1-25, CnMc7-37 once a week. Not all colonies were large enough to get pieces for all four treatments, thus sample sizes are lower for some treatments. All colonies were monitored and photographed over 28 days and the percentage of healthy tissue remaining over time was calculated (Fig. 13A). The resulting area under the curve (AUC) was compared between treatments (Fig. 13B). As healthy tissue on each fragment was measured every other day, there were gaps in the data between days where tissue was measured, so mixed effects ANOVA was conducted ($p = 0.671$). A log-rank (Mantel-Cox) test was conducted to compare the probability of survival between treatments over time (Fig. 13; $p = 0.927$). Differences between treatments were not statistically significant and CnMc7-37 and McH1-25 did not perform better than the control. Therefore, we do not plan to continue investigating the effectiveness of CnMc7-37 in the future.

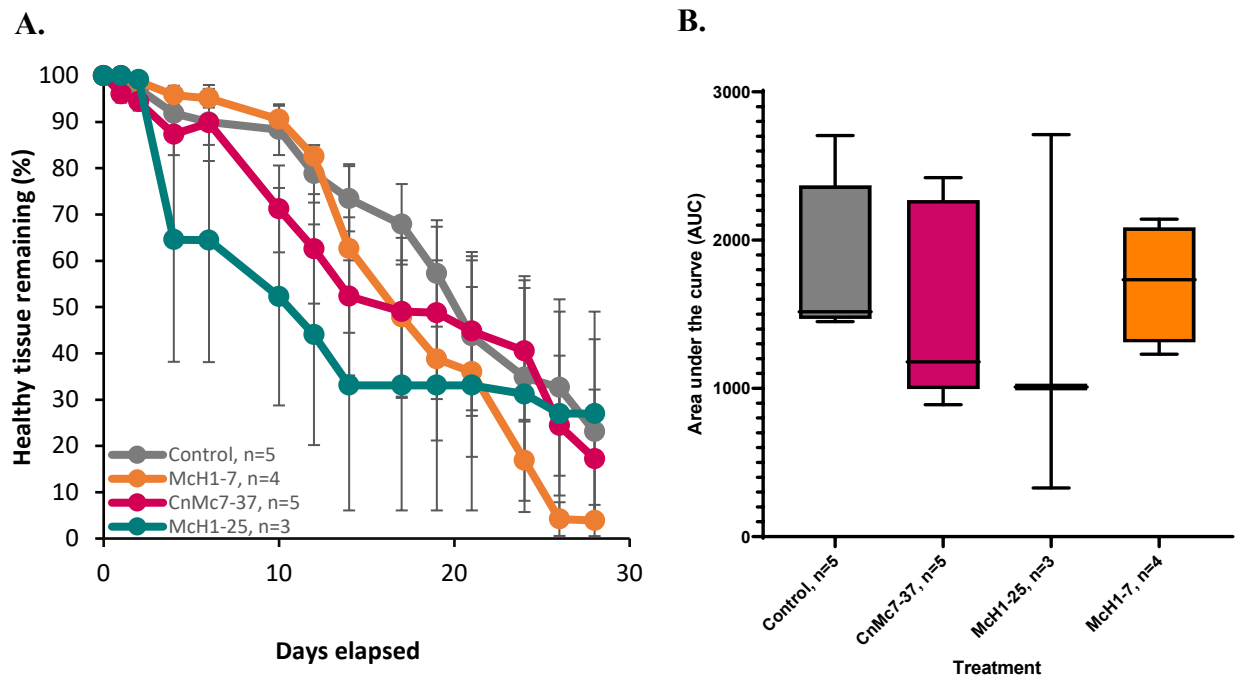


Figure 13. A) Percentage of healthy tissue remaining on infected *M. cavernosa* fragments treated with McH1-25, CnMc7-37, McH1-7, or FSW (control) and B) subsequent AUC with a larger AUC corresponding to slower disease progression. Data in A are shown as mean \pm 1 SEM. The boxes in B extend from the 25th to 75th percentiles with midline representing the median of the data. Whiskers extend from minimum to maximum of the data.

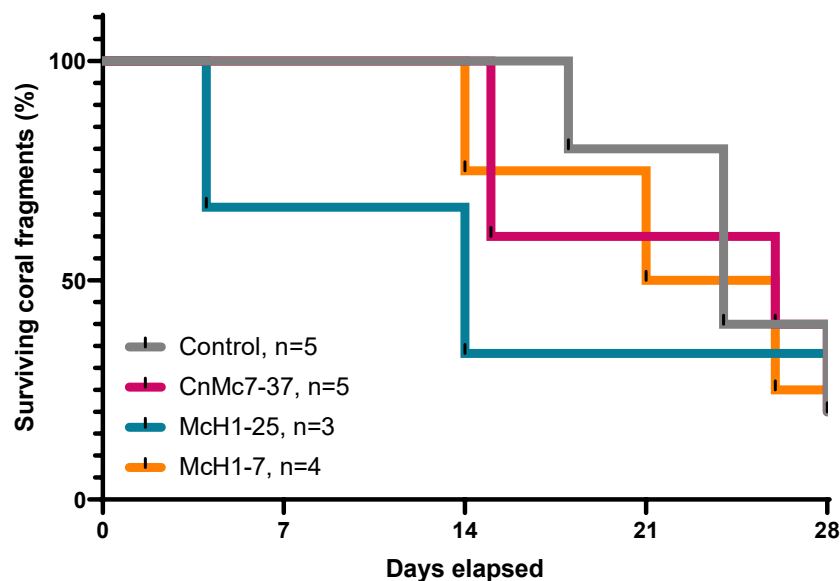


Figure 14. Analysis of the probability of survival of diseased *M. cavernosa* fragments of the same genotypes treated with McH1-25, CnMc7-37, McH1-7, or FSW (control) over time.

Effectiveness of probiotic strains D12H-1, D12H-2.2, and Of5H-5 at treating infected Orbicella faveolata and Orbicella annularis colonies

Two potential probiotic strains, D12H-1 and D12H-2.2, isolated from healthy *Diploria labyrinthiformis* colonies, as well as one strain, Of5H-5, isolated from a healthy *Orbicella faveolata* colony, produced zones of inhibition against putative pathogens and were therefore trialed in the laboratory. A total of 6 *O. faveolata* and 2 *O. annularis* colonies were fragmented to be inoculated with filtered seawater (control) or one of these three strains once a week, although not all genotypes were large enough to cut into pieces to treat all of them with all the probiotics. All colonies were monitored and photographed over 32 days and the percentage of healthy tissue remaining over time was calculated (Fig. 15A). The resulting area under the curve (AUC) was compared between treatments (Fig. 15B). As healthy tissue on each fragment was measured every other day, mixed effects ANOVA was conducted ($p = 0.54$). A log-rank (Mantel-Cox) test was conducted to compare the probability of survival between treatments over time (Fig. 15; $p = 0.499$).

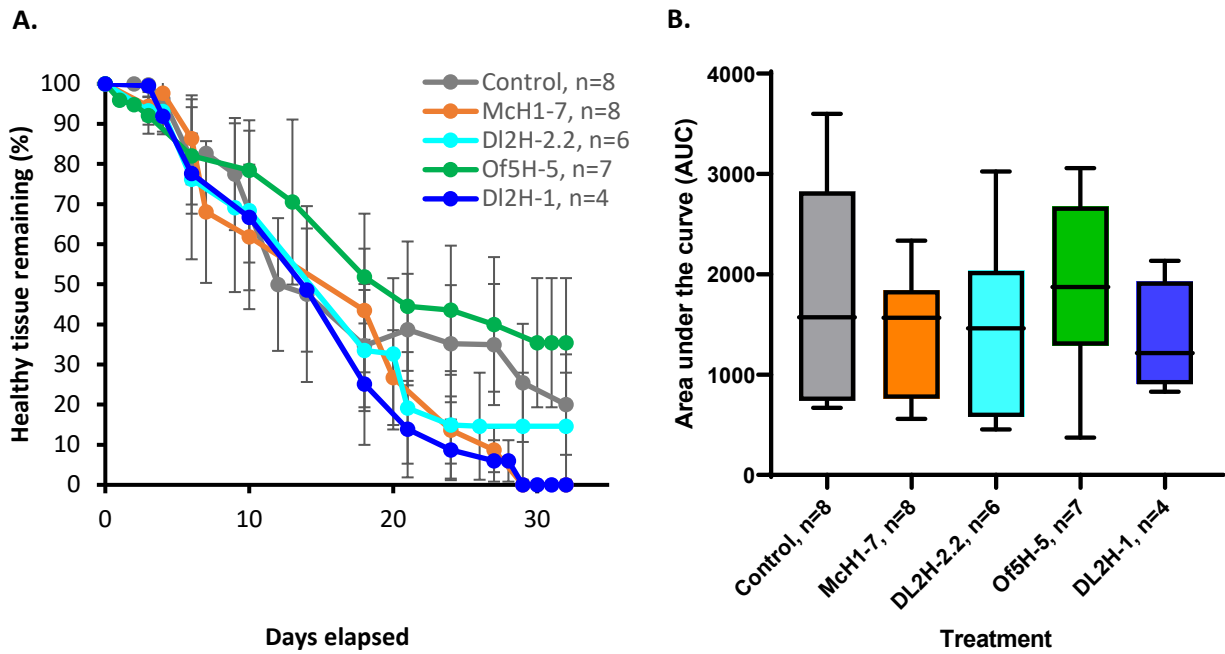


Figure 15. A) Percentage of healthy tissue remaining on infected *O. faveolata* and *O. annularis* fragments treated with DL2H-1, DL2H-2.2, Of5H-5, or FSW (control) and B) subsequent AUC with a larger AUC corresponding to slower disease progression. Data in A are shown as mean \pm 1 SEM. The boxes in B extend from the 25th to 75th percentiles with midline representing the median of the data. Whiskers extend from minimum to maximum of the data.

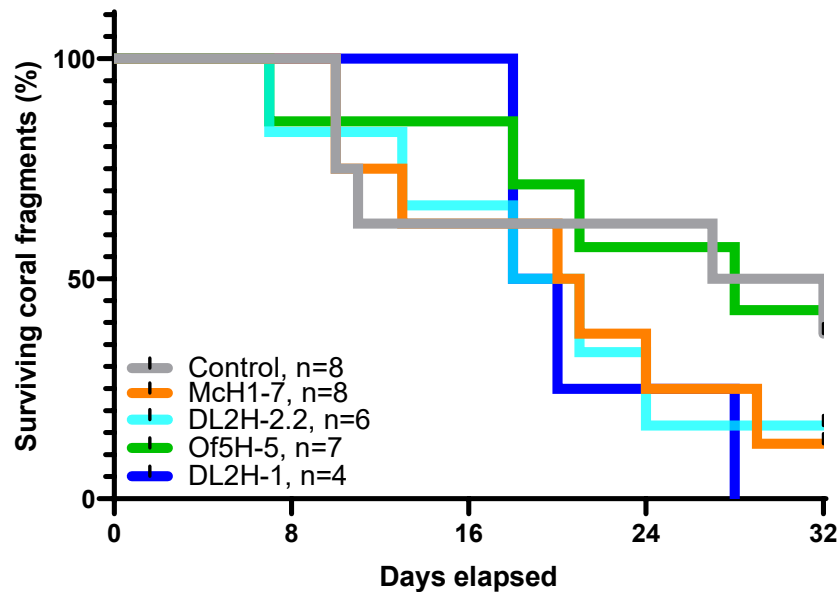


Figure 16. Analysis of the probability of survival of 6 *O. faveolata* and 2 *O. annularis* diseased fragments of the same genotypes treated with DL2H-1, DL2H-2.2, Of5H-5, or FSW (control) over time.

The *O. annularis* were removed from the analysis to determine if differences in species were driving results. Therefore, the percentage of healthy tissue remaining over time was calculated on 6 *O. faveolata* colonies (Fig. 17A). The resulting area under the curve (AUC) was compared between treatments by mixed effects ANOVA ($p = 0.373$) (Fig. 17B). A log-rank (Mantel-Cox) test was conducted to compare the probability of survival between treatments over time (Fig. 18; $p = 0.528$). Differences were not statistically significant; however, the trend for Of5H-5 was favorable, and this strain may warrant further testing. We plan to continue investigating the effectiveness of Of5H-5 in the future in comparison with other *O. faveolata* strains.

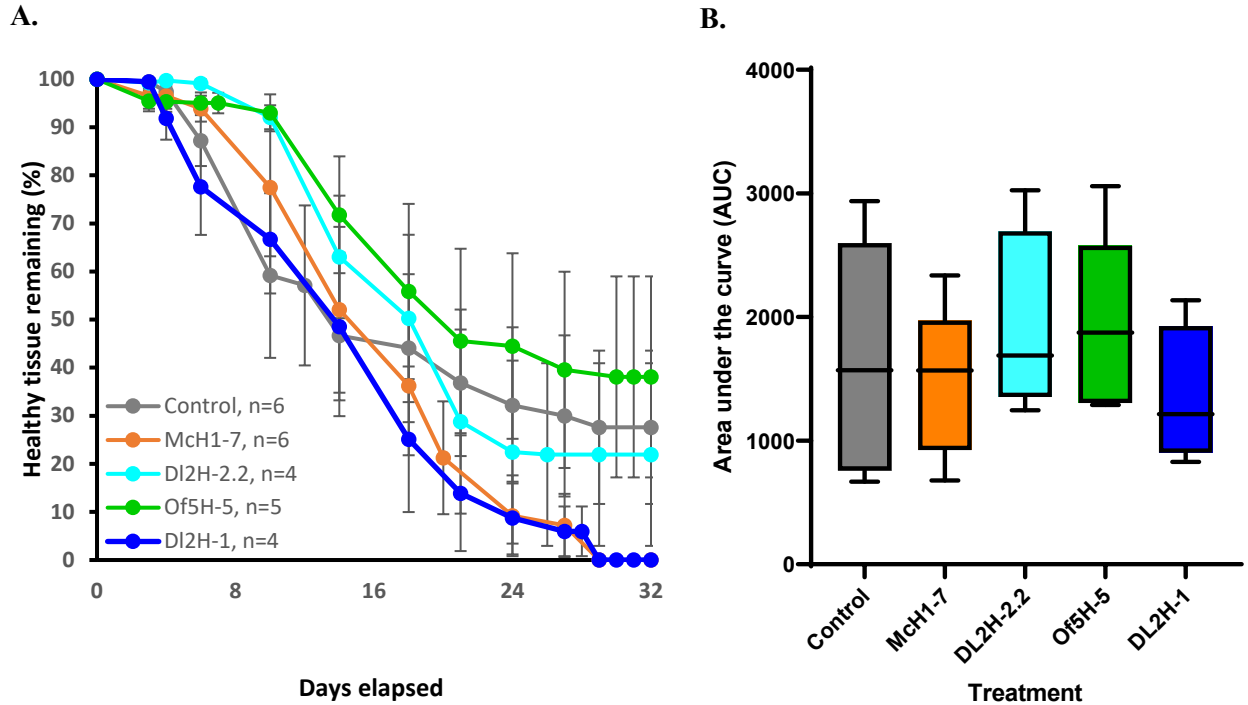


Figure 17. A) Percentage of healthy tissue remaining on infected *O. faveolata* fragments treated with DL2H-1, DL2H-2.2, Of5H-5, or FSW (control) and B) subsequent AUC with a larger AUC corresponding to slower disease progression. Data in A are shown as mean \pm 1 SEM. The boxes in B extend from the 25th to 75th percentiles with midline representing the median of the data. Whiskers extend from minimum to maximum of the data.

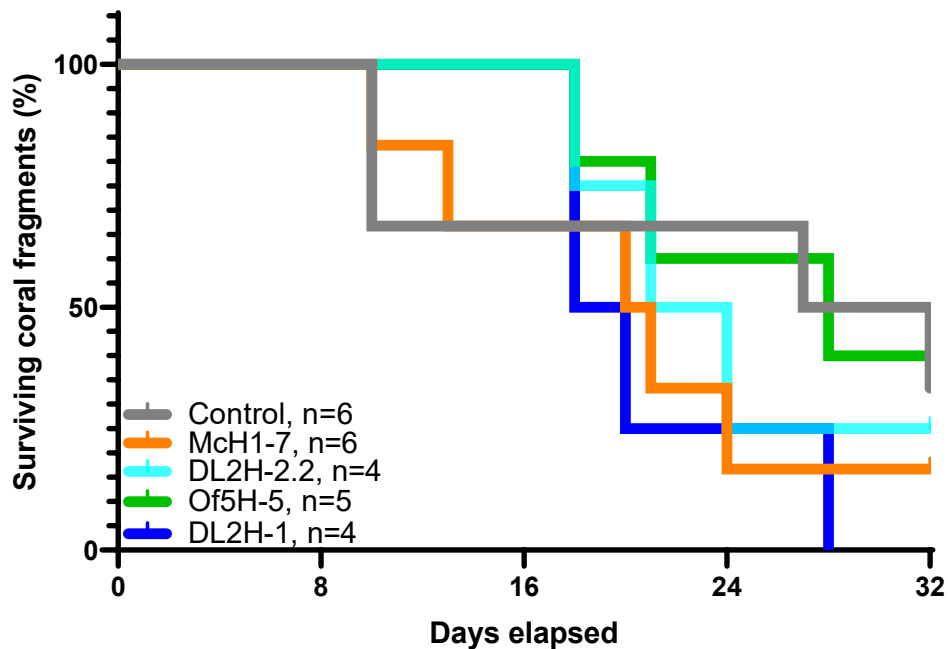


Figure 18. Analysis of the probability of survival of 6 diseased *O. faveolata* fragments of the same genotypes treated with DL2H-1, DL2H-2.2, Of5H-5, or FSW (control) over time.

Effectiveness of probiotic strains CNAT2-18.1 and CnH1-48 at treating infected Colpophyllia natans colonies

Two potential probiotic strains of isolated from healthy *C. natans* colonies, *Pseudoalteromonas ruthenica* CNAT2-18.1 and *Pleionea mediterranea* CnH1-48, produced zones of inhibition against putative pathogens and were therefore trialed on *C. natans* colonies. A total of 8 colonies were fragmented to be inoculated with filtered seawater (control) or one of these two strains once a week, although not all colonies were large enough for all treatments. All colonies were monitored and photographed over 21 days and the percentage of healthy tissue remaining over time was calculated (Fig. 19A). The resulting area under the curve (AUC) was compared between treatments (Fig. 19B) by mixed effects ANOVA ($p = 0.076$). A log-rank (Mantel-Cox) test was conducted to compare the probability of survival between treatments over time (Fig. 20; $p = 0.002$). Individual log rank (Mantel-Cox) tests were conducted between two treatments to compare differences. Tissue loss on corals treated with CNAT2-18.1 significantly differed from control ($p=0.002$) and McH1-7 ($p=0.047$) treated corals. Tissue loss on corals treated with CnH1-48 significantly differed from control treated corals ($p=0.0119$). We plan to continue investigating the effectiveness of these two strains in the future and advance them to field testing after safety testing with other coral species.

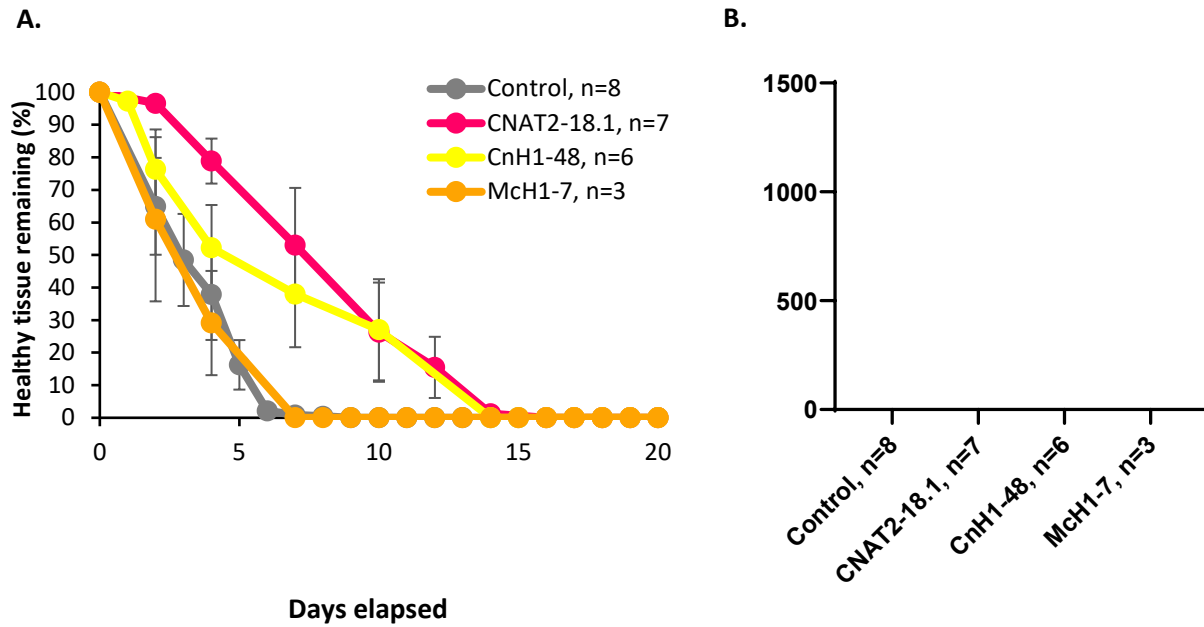


Figure 19. A) Percentage of healthy tissue remaining on infected *C. natans* fragments treated with CNAT2-18.1, CnH1-48, or FSW (control) and B) subsequent AUC with a larger AUC corresponding to slower disease progression. Data in A are shown as mean \pm 1 SEM. The boxes in B extend from the 25th to 75th percentiles with midline representing the median of the data. Whiskers extend from minimum to maximum of the data.

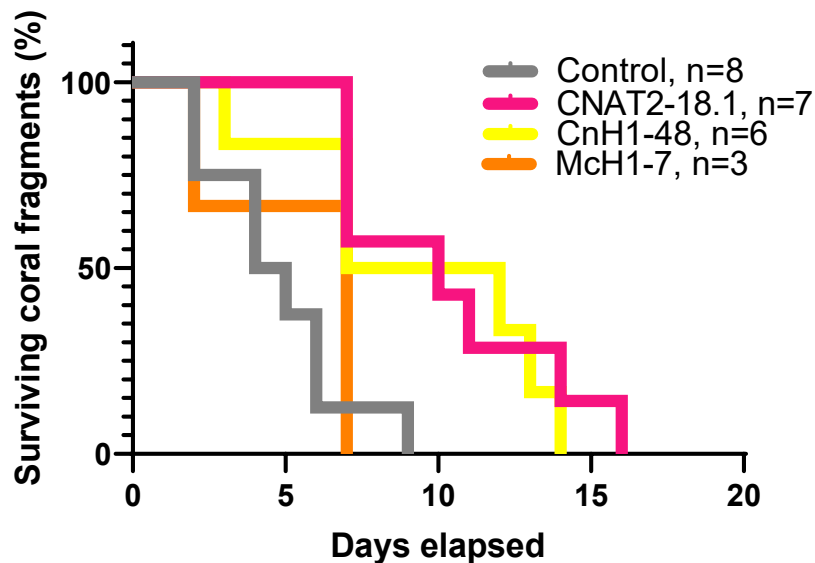


Figure 20. Analysis of the probability of survival of diseased *C. natans* fragments of the same genotype treated with CNAT2-18.1, CnH1-48, or FSW (control) over time.

To test combinational treatments of different probiotic strains on a wider variety of diseased coral species.

Utilizing a mix of probiotic strains to treat corals with SCTLD may allow for increased efficacy of probiotic strains as well as reduce the potential of pathogens evolving resistance against them.

The first step for assessing whether different strains can be combined together for treatment is to test for antagonism between strains in culture. Forty two of our active strains have now been examined in these antagonism assays by testing them against the potential probiotic strains McH1-7, CnMc7-37, DL2H-2.2, DL2H-1 and Cnat2-18. Therefore, we have the necessary information to determine which strains do not negatively interact with one another and can be combined for further testing with corals in aquaria.

Combinations of strains are currently being tested on corals in the laboratory. CnMc7-13, isolated from a healthy *M. cavernosa* colony, is currently being trialed on 3 *M. cavernosa* colonies. At the same time, strain CnMc7-15, also isolated from a healthy *M. cavernosa* colony, is being trialed on 6 *M. cavernosa* colonies. Both strains have been combined to test on 3 corals simultaneously. In addition, strain SSH13-30, isolated from a healthy *Siderastrea siderea*, is currently being trialed on 3 colonies of *S. siderea*. A second strain isolated from *S. siderea*, SSH1-16, is also being trialed on one *S. siderea* colony. Both strains have been combined to be tested on one colony of *S. siderea* in aquarium trials. All four strains showed zones of inhibition against putative pathogens in previous testing and therefore may be effective probiotics.

To characterize effective probiotics with complete genome sequencing and chemical analysis before potential deployment in the field.

Organic Extraction and C18 Separation:

A total of 102 extracts were obtained from potential probiotic strains that were grown in pans with seawater agar and the cells were harvested after 48 hrs for extraction. For all extracts, the bacterial cells were extracted with a 2:2:1 ethyl acetate:methanol:water solvent mixture to obtain the widest breadth of compounds and a crude extract of each of the strains was obtained. For 33 strains, the bacterial cells were handled in two ways prior to extraction; they were extracted wet and lyophilized (freeze dried). The purpose of this was to determine if the handling methods led to different chemistry being observed by LC-MS, either because of more efficient extraction after freeze drying or because of loss of volatile or unstable compounds.

Four strains were also grown in two, 1L flasks of seawater broth-based medium and the cells were obtained for extraction and separation: *Pseudoalteromonas rubra* (internal ID: DL2H-2.2), *Pseudoalteromonas ruthenica* (ID: CNAT2-18), *Pseudoalteromonas* sp. (internal ID: CnMC7-37), and *Pleionea mediterranea* (ID: CnH1-48). Bacterial cells were centrifuged down to a pellet and lyophilized for complete dryness. After extraction in 2:2:1 ethyl acetate:methanol:water, the crude extracts were then subjected to a column separation step, in order to implement bioactive-guided fractionation. Each extract was solubilized in methanol and placed on 300 mg of C18 (reverse-phase chromatography) resin. The solvent was removed from the extract-resin mixture before being placed on a packed C18 column (3g). Each extract was subjected to the same solvent mixtures, and the fractions were as followed: Fraction 1 (100% water, most polar), Fraction 2 (70% water: 30% acetonitrile), Fraction 3 (70% acetonitrile: 30% water), Fraction 4 (100% acetonitrile), and Fraction 5 (100% ethyl acetate, most non-polar). Fraction 1 contained mostly salts and was not tested in further assays.

Disk Diffusion of Probiotic Chemistry:

Extracts of each active strain with their respective fractions, fractions 2 to 5, were further tested in disk diffusion assays using two isolated *Vibrio coralliilyticus* strains (internal ID: OfT6-21 and OfT7-21). Extracts and fractions were tested at 31.25 mg/mL and dosed on the paper disks at 4.0 μ L (125 μ g), in triplicates. A methanol disk (solvent vehicle for assays) and paper disk only were used as the controls, respectively. Each *V. coralliilyticus* strain was seeded at an optical density of 0.500 onto the disk diffusion agar plates, before placing disks with chemistry. The plates with the strains and disks incubated for exactly 24 hours before scoring, or measuring zones of inhibition (ZOI). Partial ZOIs were scored if the zone was observed to have a cloudy appearance, while complete ZOIs were scored if the zone was observed to be clear (Figure 21).

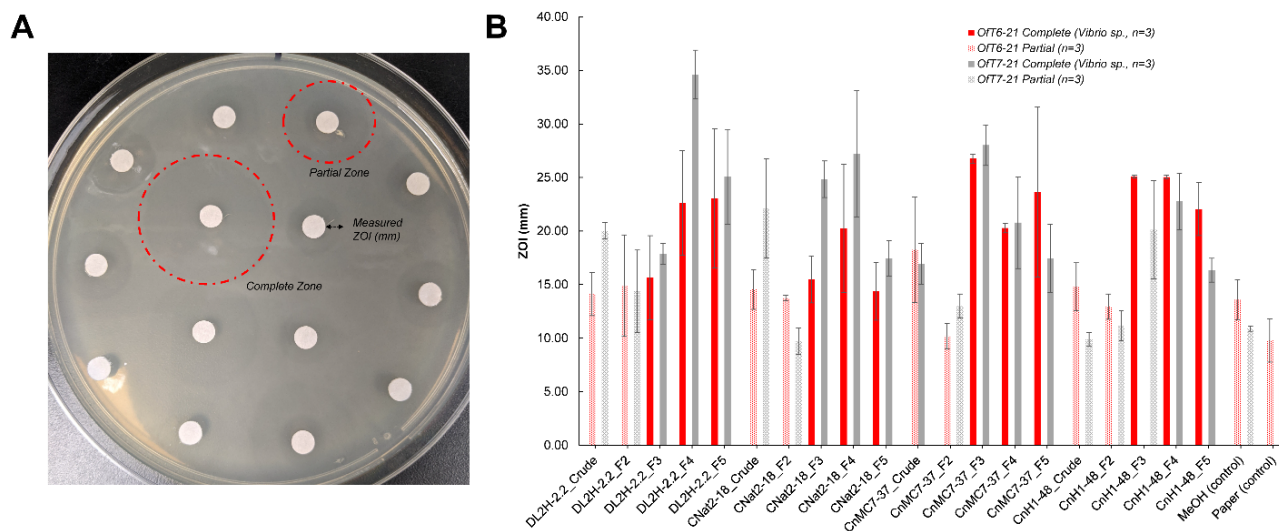


Figure 21. A) The plate layout of disk diffusion assays with OfT6-21 and OfT7-21, which 12 samples plus two control can fit. Red circles indicate what is scored a partial versus complete zone of inhibition and black arrow is how the ZOI is measured; B) ZOIs of each inhibitory bacteria extract and their respective fractions with standard error bars (n=3).

An additional 138 crude extracts were tested in the disk diffusion assays by the same methods (see Fig. 21A). Of these, 33 extracts showed large zones of inhibition and were sent to Dr. Neha Garg at Georgia Tech for follow-up studies by LC-MS.

High Resolution LC-MS Analysis:

All samples were stored at -20 °C until data was acquired by LC-MS in the laboratory of Dr. Neha Garg. All dried extracts were resuspended in 80% methanol in water (LC-MS grade) containing 1 μ M of sulfadimethoxine as an internal standard. The samples were analyzed with an Agilent 1290 Infinity II UHPLC system (Agilent Technologies) using a Kinetex 1.7 μ m C18 reversed phase UHPLC column (50 \times 2.1 mm) coupled to an ImpactII ultrahigh resolution Qq-TOF mass spectrometer (Bruker Daltonics, GmbH, Bremen, Germany) equipped with an ESI source for MS/MS analysis. A Kinetex 1.7 μ m C18 reversed phase UPLC column (50 \times 2.1 mm) was employed for chromatographic separation. MS spectra were acquired in positive ionization mode, m/z 50–2000 Da. An active exclusion of two spectra was used, implying that an MS¹ ion would not be selected for fragmentation after two consecutive MS² spectra had been recorded for it in a 0.5 min time window. The eight most intense ions per MS¹ spectra were selected for

further acquisition of MS² data. The chromatography solvent A: water + 0.1% v/v formic acid and solvent B: MeCN + 0.1% v/v formic acid were employed for the separation gradient. Flow rate was held constant at 0.5 mL/min throughout the run.

Vendor software was used to convert the raw data to mzXML format and preprocessed on MZmine 2.53 using mass detection, chromatogram building, chromatogram deconvolution, isotopic grouping, retention time alignment, duplicate removal, and missing peak filling¹. This processed data was submitted to the feature-based molecular networking workflow on the Global Natural Product Social Molecular Networking (GNPS) platform. Herein, the output of MZmine includes information about LC-MS features across all samples containing the *m/z* value of each feature, retention time of each feature, the area under the peak for the corresponding chromatogram of each feature, and a unique identifier. The MS² spectral summary contains a list of MS² spectra, with one representative MS² spectrum per feature. The mapping information between the feature quantification table and the MS² spectral summary was stored in the output using the unique feature identifier and scan number, respectively. This information was used to relate LC-MS feature information to the molecular network nodes. The quantification table and the linked MS² spectra were exported using the GNPS export module¹⁻³. Feature Based Molecular Networking was performed using the MS² spectra (mgf file) and the quantification table (csv file).

To generate the FBMN, the data was filtered by removing all MS/MS fragment ions within +/- 17 Da of the precursor *m/z*. MS/MS spectra were filtered by choosing only the top 6 fragment ions in the +/- 50 Da window throughout the spectrum. The precursor ion mass tolerance was set to 0.02 Da and the MS/MS fragment ion tolerance to 0.02 Da. A molecular network was then created where edges were filtered to have a cosine score above 0.7 and more than 4 matched peaks. Further, edges between two nodes were kept in the network if and only if each of the nodes appeared in each other's respective top 10 most similar nodes. Finally, the maximum size of a molecular family was set to 100, and the lowest scoring edges were removed from molecular families until the molecular family size was below this threshold. The spectra in the network were then searched against GNPS spectral libraries^{3,4}. The library spectra were filtered in the same manner as the input data. All matches kept between network spectra and library spectra were required to have a score above 0.7 and at least 4 matched peaks. The molecular networks were visualized using Cytoscape⁵. The compound annotations follow the "level 2" annotation standard based upon spectral similarity with public spectral libraries or spectra published in the literature as proposed by the Metabolomics Society Standard Initiative⁶.

Prior to statistical analysis, blank subtraction was performed on the quantification table using a Jupyter notebook, available at <https://github.com/Garg-Lab/Jupyter-Notebook-Blank-Subtraction/blob/main/Probiotic%20Extracts%205.29.21%20pos%20mode.ipynb>. The mean of each feature in the samples is compared separately to the mean of the feature in the solvent controls, media controls, and LC-MS blanks. A feature is retained if its sample mean is greater than 0.25 × the mean of the sample in the blanks. The entire quantification table is exported, with each feature marked as "true" (feature is retained) or "false" (feature is not retained). Visualization of the molecular network, metadata mapping, and feature filtering was performed using Cytoscape (v 3.7.2)⁵. Within Cytoscape, node filtering was performed using metadata and quantification tables and the nodes corresponding to features present in blank were removed. Statistical analysis was performed using PLS Toolbox on Matlab R2019b. Prior to statistical

analysis the data was preprocessed using pareto scaling and Ward's Method was used to generate the hierarchical clustering analysis.

Additional compound annotations were performed using the *in-silico* tool MolDiscovery (v.1.0.0). MolDiscovery, available through the GNPS platform, compares *in silico* generated mass spectra of small molecules from a variety of databases with experimental MS² spectra and includes a similarity score for each reported match⁷. The LC-MS feature list exported from MZmine was submitted to the MolDiscovery workflow.

Tocomonoenol

The annotation of tocomonoenol was suggested by MolDiscovery. We previously ran a standard of alpha-tocopherol using the same LC-MS method employed above. Comparing the MS² spectra of the feature *m/z* 429.372 (top) and the standard (bottom) supports the annotation of *m/z* 429.372 as a tocomonoenol (Figure 22). The feature was only detected in the lyophilized extract of Ofav3-42 *Ruegeria atlantica*, which showed activity against *Vibrio coralliilyticus* OFT6-21 and OFT7-21 in the disk diffusion assay. Interestingly, tocopherols are thought to only be synthesized by photosynthetic organisms^{8,9}, which *Ruegeria atlantica* is not. Tocomonoenol and other tocopherols have reported antioxidant activity.^{10,11}

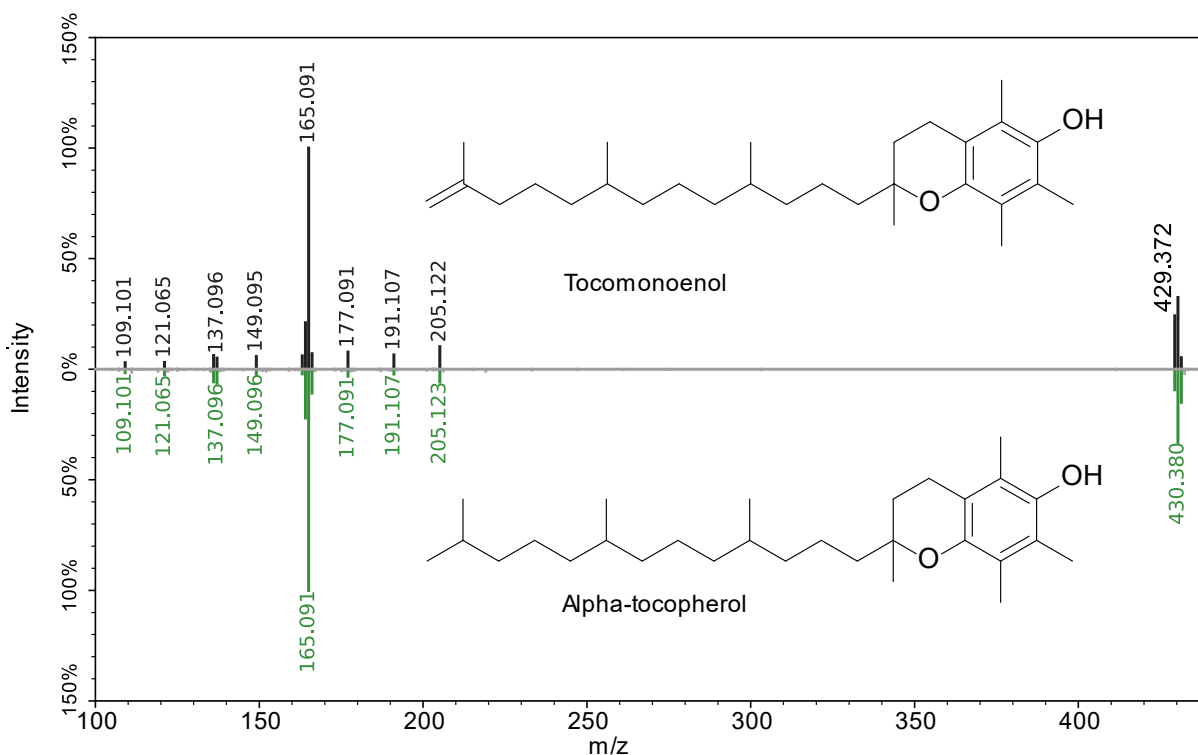


Figure 22. Mirror plot of MS² spectra of tocomonoenol present in Ofav3-42 *Ruegeria atlantica* (top spectra) and the analytical standard of alpha-tocopherol (bottom spectra).

Ngercheumicins

Another set of annotations proposed by MolDiscovery and confirmed with MS² annotations were ngercheumicin G (*m/z*_RT 855.579_12.8) and ngercheumicin I (*m/z*_RT 833.610_13.9). These

cyclic peptides have been previously isolated from a marine *Photobacterium* related to *P. halotolerans*.¹² Ngercheumicin G showed inhibition of genes associated with *agr* quorum sensing in *S. aureus* (ngercheumicin I did not show significant inhibition at the concentrations tested).¹² The annotated features clustered with seven other nodes, all of which were annotated as ngercheumicin related compounds with identical macrolide structures (the modifications were within the acyl tail). The m/z_RT (retention time, min) are included in Figure 23. These features were only detected in bacterial isolates CnH1-48, Cnat2-18, and Cnat2-41, two of which were tested on live corals and slowed progression of SCTLD (Figs. 19, 20). The bacterial strains these features were detected in include *Pleionea mediterranea* (CnH 1-48) and the other two strains were identified as *Pseudoalteromonas ruthenica*. These bacterial extracts showed activity against *Leisingera* sp. and *Vibrio coralliilyticus*. Further studies should indicate if these compounds are inhibiting or interfering with quorum sensing in gram negative bacteria.

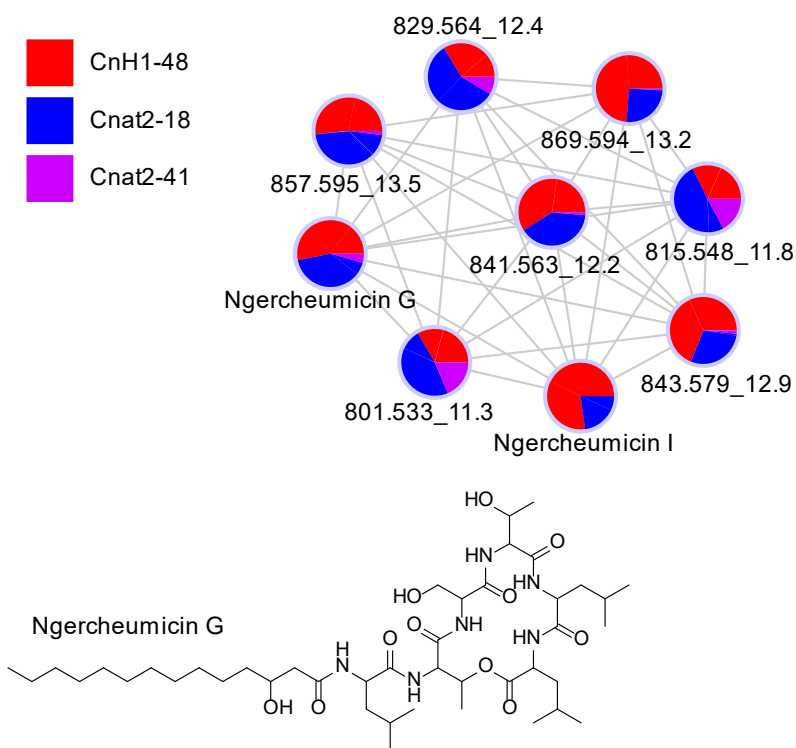


Figure 23. Network analysis of mass spectral features of the ngercheumicins found in three probiotic strains isolated from *Colpophyllia natans*, CnH1-48, Cnat2-18, and Cnat2-41.

Prodigiosin and Analogs

Pseudoalteromonas rubra strain DL2H-2.2 was highly active in the disk diffusion assay and was analyzed to determine the active metabolites. Previously reported, *P. rubra* was isolated from Indonesian seawater and its metabolites were identified as cycloprodigiosin that exhibited broad-band antibacterial activity, prodigiosin responsible for the red pigment, and four prodiginine analogs only differing in their alkyl chain length.¹³ The *Diploria labyrinthiformis* derived *P.*

rubra produces the antibiotic, cycloprodigiosin, (m/z 322.1905, Δppm -2.76) as well as prodigiosin as the main metabolite (m/z 324.2069, Δppm -0.43). The metabolites were confirmed by EIC for the calculated m/z values with a low error as well as retention time observations, as observed by Brotosudarmo and authors.¹³ Three out of the four prodiginine analogs were confirmed by their respective m/z . 2-methyl-3-hexyl-prodiginine was observed to be a major metabolite along with cycloprodigiosin and prodigiosin, which was also observed in the *D. labyrinthiformis* derived *P. rubra* strain (m/z 338.2227, Δppm 0.03). 2-methyl-3-butyl prodiginine (m/z 310.1905, Δppm -2.87) and 2-methyl-3-heptyl-prodiginine (m/z 352.2384, Δppm 0.17) were also confirmed in the EIC analysis (Fig. 24).

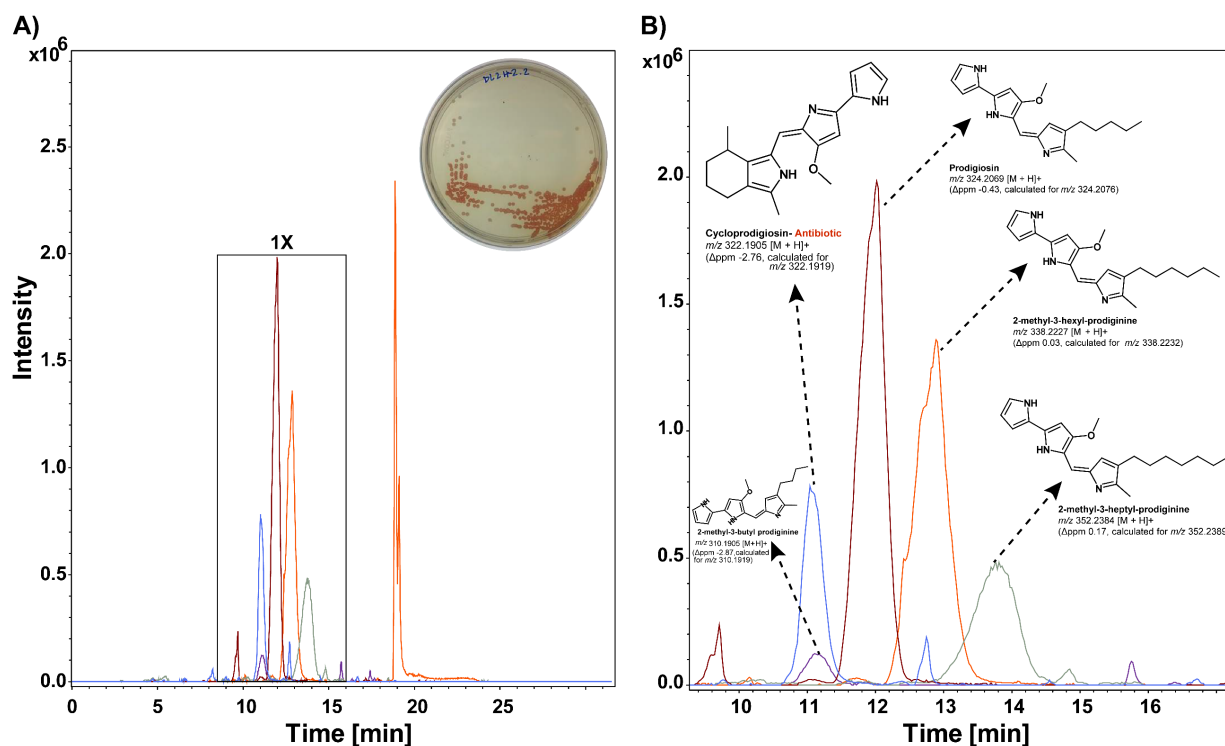


Figure 24. A) Extracted ion chromatogram (EIC) of *P. rubra* DL2H-2 with five known metabolites identified via m/z ; B) 1X inset of the EIC intensities of the identified metabolites with their respective m/z values compared to their theoretical m/z and calculated error in Δppm .

Prodigiosin, cycloprodigiosin, and structural analogs of prodigiosin including 2-methyl-3-hexyl prodiginine, 2-methyl-3-butyl prodiginine, and 2-methyl-3-heptyl prodiginine were detected in several strains of *Pseudoaltermonas rubra*. All annotations were confirmed using MS² annotation. The other nodes within this network are labeled with m/z _RT (retention time, min) (Fig. 25).

m/z _RT of all nodes reported with a name:

Prodigiosin: 324.207_12.1

Cycloprodigiosin: 322.191_11.3

2-Methyl-3-hexyl prodiginine: 338.223_13.0

2-Methyl-3-butyl prodiginine: 310.191_11.1

2-Methyl-3-heptyl prodiginine: 352.238_13.8

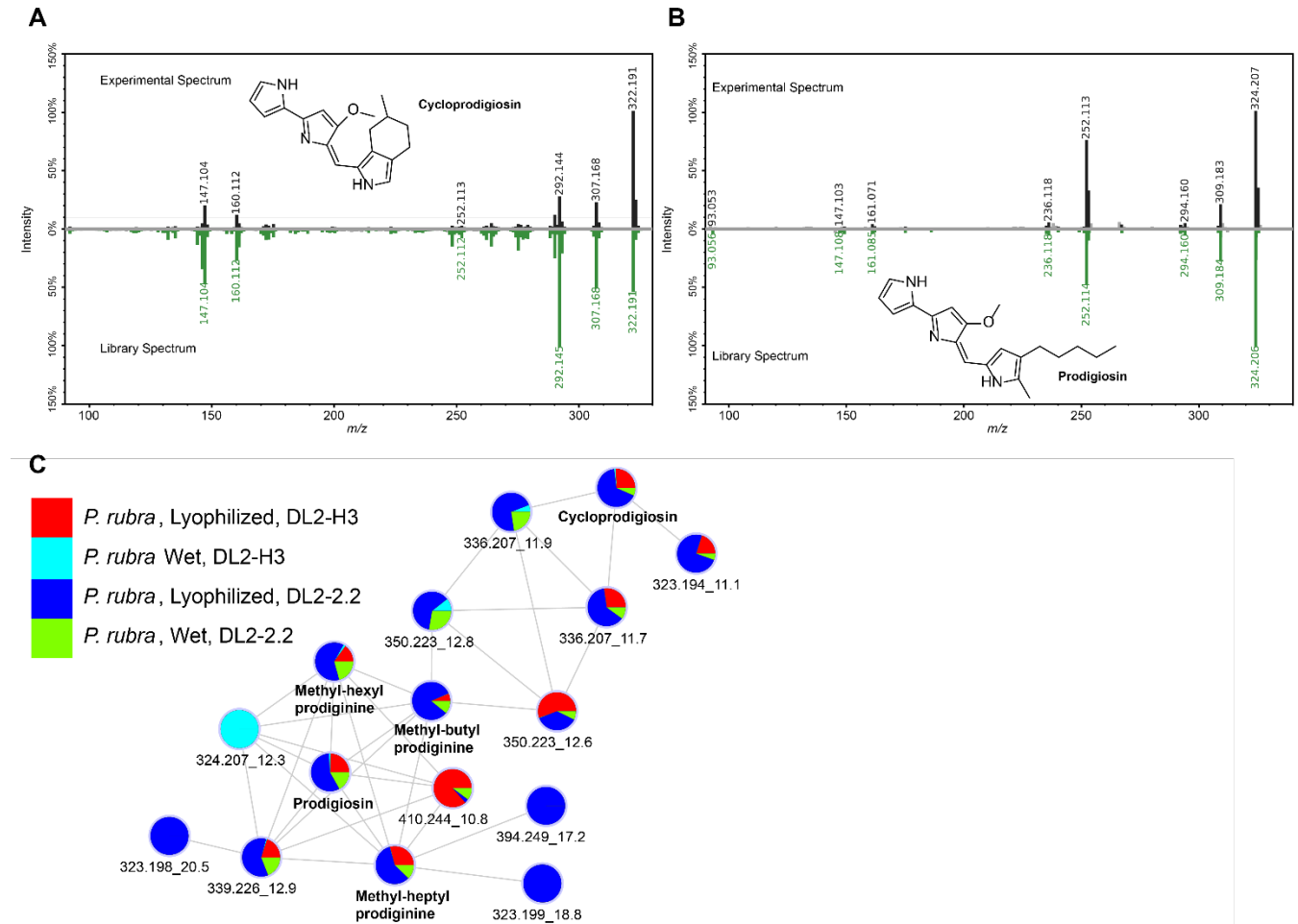


Figure 25. Mirror match plot of feature with m/z_RT 322.191_12.3 (top) and GNPS library spectrum of cycloprodigiosin (bottom). (B) mirror match plot of feature with m/z_RT 324.207_12.1 (top) and GNPS library spectrum of prodigiosin (bottom). (C) Cluster of prodigiosin, cycloprodigiosin, and structural analogs of prodigiosin including 2-methyl-3-hexyl prodiginine, 2-methyl-3-butyl prodiginine, and methyl-heptyl prodiginine.

HCA plot

The hierarchical clustering analysis of the LC-MS metabolomics data revealed several species within this study clustered closely together. A small weighted difference between two samples indicates similarity between the metabolomes of these samples. The colored lines show instances where the same bacterial strains cluster together as the most similar bacterial extracts. For some strains, including *Tenacibaculum aiptasiae*, *Vibrio coralliilyticus*, *Vibrio alginolyticus*,

Pseudoalteromonas rubra, and *Pseudoalteromonas piscicida*, the extraction method influenced the clustering pattern (LYO= lyophilized extraction, Wet= wet extraction) (Fig. 26). This is of interest as we try to develop the best extraction methods for samples going forward. We will further determine if compounds are being lost or more efficiently extracted with one method or the other to better understand the biosynthetic capacity of these potential probiotic strains.

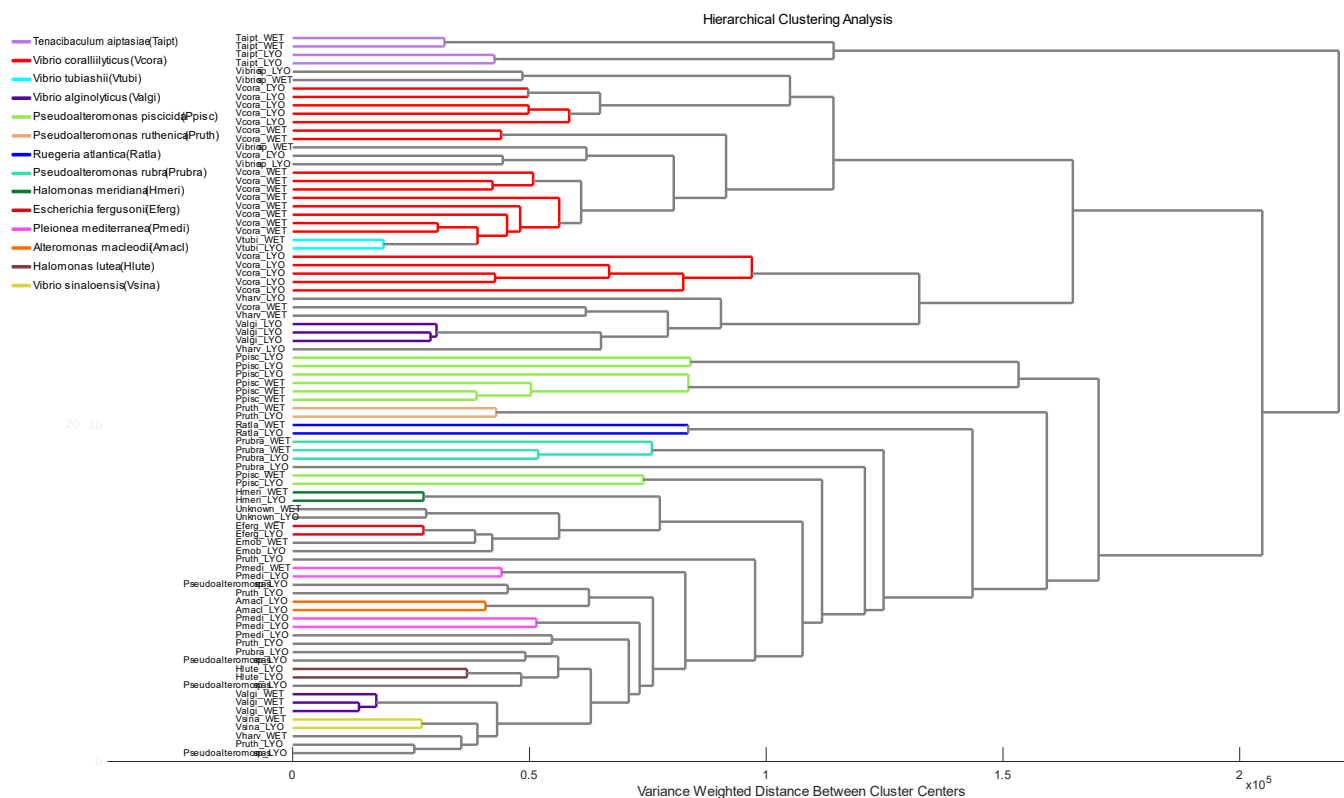


Figure 26. Hierarchical clustering analysis of the LC-MS metabolomics data for 86 extracts of coral-derived bacteria. These strains were extracted wet and lyophilized for comparison of best methods for extraction. Note that clustering occurs based on extraction methods indicating that differences are occurring based on method.

Task #3: To develop and test diagnostic tools to complement probiotic treatments.

To screen diseased corals using the immunological assays specific to *V. coralliilyticus* to assess the potential threat posed by the pathogen and interference with probiotic treatment.

The role of *Vibrio coralliilyticus* in SCTLD infections has been investigated since 2018. The presence of this bacterium on corals with faster progressing disease suggests its role in secondary or coinfections of SCTLD. To continue the investigation of the role of *V. coralliilyticus* on infected corals, all corals being brought into the laboratory for use in experiments have been tested for the presence of VcpA, a toxic metalloprotease produced by pathogenic strains of this bacterium using the *Vibriosis VcpA RapidTest* (mAbDx, Inc.). All corals collected between July

2020 and June 2021 including 19 *M. cavernosa*, 18 *C. natans*, 8 *S. siderea*, 2 *Pseudodiploria strigosa*, 2 *O. annularis*, and 1 *D. labyrinthiformis* colonies from the Florida Keys have tested negative for VcpA. In addition, 2 *M. cavernosa* and 1 *O. faveolata* colonies from Fort Lauderdale also tested negative from VcpA.

An investigation of the impact of the presence of *V. coralliilyticus* on the effectiveness of McH1-7 in the lab was conducted from 2019-2020. McH1-7 was not as effective at treating corals with SCTLD that were positive for VcpA. Therefore, corals at BS2 were tested for the presence of *V. coralliilyticus* to determine if this bacterium was impacting McH1-7 effectiveness in the field. A total of 24% of corals at BS2 were VcpA+ (Table 2). Of the 9 corals that tested positive for VcpA, 6 have actively progressing disease. Interestingly, the 3 corals treated with a probiotic bag that tested positive for VcpA did not have actively progressing disease, suggesting that *V. coralliilyticus* may not impede the ability of McH1-7 to stop SCTLD. However, a greater sample size is required to determine if this trend is accurate.

Table 2. Total corals treated at BS2 that were VcpA+.

Treatment	Total corals treated	Total corals VcpA+
Probiotic paste	10	1
Probiotic bag	9	3
Control paste	9	3
Control bag	8	1
Background control	5	2
Total:	41	9

Zero corals at Mk48-5 in the Florida Keys were positive for VcpA suggesting that the presence of *V. coralliilyticus* may be seasonal or may only have established on specific reefs throughout Florida's Coral Reef.

To screen diseased corals for other pathogenic strains that interfere with probiotic treatment.

We have developed methods to grow anaerobic bacteria from diseased corals using a small anaerobic chamber as well as an airtight container and candle to exhaust oxygen within. Microbiome analysis suggests that some of the anaerobic bacteria such as *Clostridia* become more prevalent in corals with SCTLD relative to uninfected corals. We recently sent six of these strains of bacteria grown in anaerobic conditions for 16S rRNA gene sequencing. Strains were identified as the anaerobe *Halodesulfovibrio* sp. and *Vibrio mediterranei*, which may be a facultative anaerobe. Testing will take place to see if these can cause increased tissue loss in corals with SCTLD.

To identify molecular markers for diseased colonies and indicators of treatment success using metabolomics for development of diagnostic tools to accompany disease treatments.

Dr. Neha Garg took the lead on a LC-MS metabolomics study using untargeted metabolomic profiling of *Montastraea cavernosa* corals affected by stony coral tissue loss disease to identify

metabolic markers of disease. Extracts from apparently healthy, diseased, and recovered corals, *Montastraea cavernosa*, collected at the BS2 reef site near Fort Lauderdale, Florida were subjected to liquid-chromatography mass spectrometry-based metabolomics. These were the untreated samples of coral mucus/tissue collected before probiotic treatments (Fig. 4). Unsupervised principal component analysis reveals wide variation in metabolomic profiles of healthy corals of the same species, which also differ from diseased corals. Using a combination of supervised and unsupervised metabolomics data analyses tools, we described metabolite features that explain variation between the apparently healthy corals, between diseased corals, and between the healthy and the diseased corals. By employing a culture-based approach, we assigned sources of a subset of these molecules to the endosymbiotic dinoflagellates, Symbiodiniaceae (colloquially called zooxanthellae). Specifically, we identify various endosymbiont-specific lipid classes, such as betaine lipids, glycolipids, and tocopherols, which differentiate samples taken from apparently healthy corals and diseased corals. Given the variation observed in metabolite fingerprints of corals, our data suggests that metabolomics is a viable approach to link metabolite profiles of different coral species with their susceptibility and resilience to numerous coral diseases spreading through the reefs worldwide. This manuscript was recently submitted to *Frontiers in Marine Science* for their special issue on Stony Coral Tissue Loss Disease.

Publications 2020-2021:

Ushijima, Blake, Meyer, Julie, Thompson, Sharon, Pitts, Kelly, Marusich, Michael F., Tittl, Jessica, Weatherup, Elizabeth, Reu Jacqueline, Wetzell, Raquel, Aeby, Greta S., Häse, Claudia, C. and Paul, Valerie J. (2020) Disease diagnostics and potential coinfections by *Vibrio coralliilyticus* during an ongoing coral disease outbreak in Florida. *Front. Microbiol.* 11:569354. [https://doi: 10.3389/fmicb.2020.569354](https://doi.org/10.3389/fmicb.2020.569354)

Traylor-Knowles, Nikki, Michael T. Connelly, Benjamin D. Young, Katherine Eaton, Erinn Muller, Valerie Paul, Blake Ushijima, Allyson DeMerlis, Melissa K. Drown, Ashley Goncalves, Nicholas Kron, Grace A. Snyder, Cecily Martin, Kevin Rodriguez. (2021) Gene expression response to Stony Coral Tissue Loss Disease transmission in *M. cavernosa* and *O. faveolata* from Florida. *Front. Mar. Sci.* doi: 10.3389/fmars.2021.681563

Deutsch, Jessica M., Olakunle Jaiyesimi, Kelly Pitts, Jay Houk, Blake Ushijima, Brian K. Walker, Valerie J. Paul, and Neha Garg. Metabolomics of healthy and stony coral tissue loss disease affected *Montastraea cavernosa* corals. *Front. Mar. Sci.* in review.

Results summary and future directions:

- Treating corals in the field with McH1-7 was effective in Fort Lauderdale with both whole colony and lesion specific techniques, but minor changes to methodology will allow for better treatment in areas with greater water movement. To our knowledge, these are the first field trials of probiotics on corals. These novel and innovative methods have management implications for treatment and prevention of SCTLD and future coral diseases.

- McH1-7 was not only able to stop disease progression on most corals treated using the bagging technique, but also allowed for the healing of bleached tissue. Using both the probiotic bag and paste technique combined may allow for greater success in the future.
- Over 100 out of ~700 new isolates show antibacterial activity against putative pathogens, including nine isolates of Actinobacteria. These will be further narrowed down for testing in aquarium assays based on taxonomy and chemical and genomic studies that suggest novel strains.
- Of5H-5, CNAT2-18-1 and CnH1-48 show promise as effective probiotics for treating corals with SCTLD. Interestingly, both CNAT2-18-1 and CnH1-48 produce known quorum sensing inhibitors, the ngeucherumicins, which may explain their probiotic activity. Further studies of their biochemistry and genomics with additional aquarium testing will allow us to proceed to field trials with these strains.
- Additional annotations of the compounds detected in untargeted metabolomics data will further enhance the knowledge of antimicrobial compounds produced by probiotic bacteria against pathogenic bacteria.
- Unsupervised methods such as HCA also allow for visualization of isolated bacteria with similar metabolomes allowing prioritization of isolates with unique metabolomics signature.
- *Vibrio coralliilyticus* did not have a strong presence on corals utilized in laboratory studies or on corals at Mk48-5 in the Keys but was found on 24% of corals at BS2 in Ft. Lauderdale. This bacterium did not appear to greatly impact the effectiveness of McH1-7 at BS2.

References Cited

1. Pluskal, T.; Castillo, S.; Villar-Briones, A.; Orešič, M., MZmine 2: Modular framework for processing, visualizing, and analyzing mass spectrometry-based molecular profile data. *BMC Bioinformatics* **2010**, *11* (1), 395.
2. Nothias, L.-F.; Petras, D.; Schmid, R.; Dührkop, K.; Rainer, J.; Sarvepalli, A.; Protsyuk, I.; Ernst, M.; Tsugawa, H.; Fleischauer, M.; Aicheler, F.; Aksenov, A. A.; Alka, O.; Allard, P.-M.; Barsch, A.; Cachet, X.; Caraballo-Rodriguez, A. M.; Da Silva, R. R.; Dang, T.; Garg, N.; Gauglitz, J. M.; Gurevich, A.; Isaac, G.; Jarmusch, A. K.; Kameník, Z.; Kang, K. B.; Kessler, N.; Koester, I.; Korf, A.; Le Gouellec, A.; Ludwig, M.; Martin H, C.; McCall, L.-I.; McSayles, J.; Meyer, S. W.; Mohimani, H.; Morsy, M.; Moyne, O.; Neumann, S.; Neuweger, H.; Nguyen, N. H.; Nothias-Esposito, M.; Paolini, J.; Phelan, V. V.; Pluskal, T.; Quinn, R. A.; Rogers, S.; Shrestha, B.; Tripathi, A.; van der Hooft, J. J. J.; Vargas, F.; Weldon, K. C.; Witting, M.; Yang, H.; Zhang, Z.; Zubeil, F.; Kohlbacher, O.; Böcker, S.; Alexandrov, T.; Bandeira, N.; Wang, M.; Dorrestein, P. C., Feature-based molecular networking in the GNPS analysis environment. *Nature Methods* **2020**, *17* (9), 905-908.
3. Wang, M.; Carver, J. J.; Phelan, V. V.; Sanchez, L. M.; Garg, N.; Peng, Y.; Nguyen, D. D.; Watrous, J.; Kapono, C. A.; Luzzatto-Knaan, T.; Porto, C.; Bouslimani, A.; Melnik, A.

V.; Meehan, M. J.; Liu, W.-T.; Crüsemann, M.; Boudreau, P. D.; Esquenazi, E.; Sandoval-Calderón, M.; Kersten, R. D.; Pace, L. A.; Quinn, R. A.; Duncan, K. R.; Hsu, C.-C.; Floros, D. J.; Gavilan, R. G.; Kleigrewe, K.; Northen, T.; Dutton, R. J.; Parrot, D.; Carlson, E. E.; Aigle, B.; Michelsen, C. F.; Jelsbak, L.; Sohlenkamp, C.; Pevzner, P.; Edlund, A.; McLean, J.; Piel, J.; Murphy, B. T.; Gerwick, L.; Liaw, C.-C.; Yang, Y.-L.; Humpf, H.-U.; Maansson, M.; Keyzers, R. A.; Sims, A. C.; Johnson, A. R.; Sidebottom, A. M.; Sedio, B. E.; Klitgaard, A.; Larson, C. B.; Boya P, C. A.; Torres-Mendoza, D.; Gonzalez, D. J.; Silva, D. B.; Marques, L. M.; Demarque, D. P.; Pociute, E.; O'Neill, E. C.; Briand, E.; Helfrich, E. J. N.; Granatosky, E. A.; Glukhov, E.; Ryffel, F.; Houson, H.; Mohimani, H.; Kharbush, J. J.; Zeng, Y.; Vorholt, J. A.; Kurita, K. L.; Charusanti, P.; McPhail, K. L.; Nielsen, K. F.; Vuong, L.; Elfeki, M.; Traxler, M. F.; Engene, N.; Koyama, N.; Vining, O. B.; Baric, R.; Silva, R. R.; Mascuch, S. J.; Tomasi, S.; Jenkins, S.; Macherla, V.; Hoffman, T.; Agarwal, V.; Williams, P. G.; Dai, J.; Neupane, R.; Gurr, J.; Rodríguez, A. M. C.; Lamsa, A.; Zhang, C.; Dorrestein, K.; Duggan, B. M.; Almaliti, J.; Allard, P.-M.; Phapale, P.; Nothias, L.-F.; Alexandrov, T.; Litaudon, M.; Wolfender, J.-L.; Kyle, J. E.; Metz, T. O.; Peryea, T.; Nguyen, D.-T.; VanLeer, D.; Shinn, P.; Jadhav, A.; Müller, R.; Waters, K. M.; Shi, W.; Liu, X.; Zhang, L.; Knight, R.; Jensen, P. R.; Palsson, B. Ø.; Pogliano, K.; Linington, R. G.; Gutiérrez, M.; Lopes, N. P.; Gerwick, W. H.; Moore, B. S.; Dorrestein, P. C.; Bandeira, N., Sharing and community curation of mass spectrometry data with Global Natural Products Social Molecular Networking. *Nature Biotechnology* **2016**, *34* (8), 828-837.

4. Jisayuki, H.; Masanoir, A.; Kanaya, S.; Nihei, Y.; Ikeda, T.; Suwa, K.; Ojima, Y.; Tanaka, K.; Tanaka, S.; Aoshima, K.; Oda, Y.; Kakazu, Y.; Kusano, M.; Tohge, T.; Matsuda, F.; Sawada, Y.; Hirai, M. Y.; Nakanishi, H.; Ikeda, K.; Akimoto, N.; Maoka, T.; Takahashi, H.; Ara, T.; Sakurai, N.; Suzuki, H.; Shibata, D.; Neumann, S.; Iida, T.; Tanaka, K.; Funatsu, K.; Matsuura, F.; Soga, T.; Taguchi, R.; Saito, K.; Nishioka, T., MassBank: a public repository for sharing mass spectral data for life sciences. **2010**, *45* (7), 1096-9888 (Electronic).

5. Shannon, P.; Markie, A.; Ozier, O.; Baliga, N. S.; Wang, J. T.; Ramage, D.; Amin, N.; Schwikowski, B.; Ideker, T., Cytoscape: A Software Environment for Integrated Models of Biomolecular Interaction Networks. *Genome Research* **2003**, *13*, 2498-2504.

6. Sumner, L. W.; Amberg, A.; Barrett, D.; Beale, M. H.; Berger, R.; Daykin, C. A.; Fan, T. W. M.; Fiehn, O.; Goodacre, R.; Griffin, J. L.; Hankemeier, T.; Hardy, N.; Harnly, J.; Higashi, R.; Kopka, J.; Lane, A. N.; Lindon, J. C.; Marriott, P.; Nicholls, A. W.; Reilly, M. D.; Thaden, J. J.; Viant, M. R., Proposed minimum reporting standards for chemical analysis Chemical Analysis Working Group (CAWG) Metabolomics Standards Initiative (MSI). *Metabolomics* **2007**, *3* (3), 211-221.

7. Cao, L.; Guler, M.; Tagirdzhanov, A.; Lee, Y.; Gurevich, A.; Mohimani, H., MolDiscovery: Learning Mass Spectrometry Fragmentation of Small Molecules. *bioRxiv* **2020**.

8. Munné-Bosch, S.; Alegre, L., The function of tocopherols and tocotrienols in plants. *Critical Reviews in Plant Sciences* **2002**, *21* (1), 31-57.

9. Grusak, M. A.; DellaPenna, D., Improving the nutrient composition of plants to enhance human nutrition and health. *Annual review of plant biology* **1999**, *50* (1), 133-161.
10. Beppu, F.; Aida, Y.; Kaneko, M.; Kasatani, S.; Aoki, Y.; Gotoh, N., Functional evaluation of marine-derived tocopherol, a minor homolog of vitamin E, on adipocyte differentiation and inflammation using 3T3-L1 and RAW264.7 cells. *Fish. Sci.* **2020**, *86* (2), 415-425.
11. Yamamoto, Y.; Maita, N.; Fujisawa, A.; Takashima, J.; Ishii, Y.; Dunlap, W. C., A new vitamin E (α -Tocomonoenol) from eggs of the pacific salmon *Oncorhynchus keta*. *J. Nat. Prod.* **1999**, *62* (12), 1685-1687.
12. Kjaerulff, L.; Nielsen, A.; Mansson, M.; Gram, L.; Larsen, T. O.; Ingmer, H.; Gotfredsen, C. H., Identification of four new agr quorum sensing-interfering cyclodepsipeptides from a marine Photobacterium. *Marine drugs* **2013**, *11* (12), 5051-5062.
13. Setiyono, E.; Adhiwibawa, M. A. S.; Indrawati, R.; Prihastyanti, M. N. U.; Shioi, Y.; Brotosudarmo, T. H. P., An Indonesian Marine Bacterium, *Pseudoalteromonas rubra*, Produces Antimicrobial Prodiginine Pigments. *ACS Omega* **2020**, *5* (9), 4626-4635.